CAPITAL UNIVERSITY OF SCIENCE AND TECHNOLOGY, ISLAMABAD

Effects of an Inclined Magnetic Field on the Unsteady Squeezing Flow between Parallel Plates with Suction/Injection

by

Ibrahim Jahangeer

A thesis submitted in partial fulfillment for the degree of Master of Philosophy

in the

Faculty of Computing
Department of Mathematics

2020

This thesis is dedicated to my beloved parents especially my mom, who helped me in my thesis and motivated me all the time.

CERTIFICATE OF APPROVAL

Effects of an Inclined Magnetic Field on the Unsteady Squeezing Flow between Parallel Plates with Suction/Injection

by

Ibrahim Jahangeer

Registration No MMT173028

THESIS EXAMINING COMMITTEE

S. No.	Examiner	Name	Organization
(a)	External Examiner	Dr. Muhammad Mushtaq	COMSATS, Islamabad
(b)	Internal Examiner	Dr. Kashif Rehman	CUST, Islamabad
(c)	Supervisor	Dr. Shafqat Hussain	CUST, Islamabad

Dr. Shafqat Hussain
Thesis Supervisor
November, 2020

Dr. Muhammad Sagheer
Head
Dept. of Mathematics
November, 2020

Dr. Muhammad Abdul Qadir
Dean
Faculty of Computing
November, 2020

Author's Declaration

I, **Ibrahim Jahangeer** hereby state that my M.Phil thesis titled "**Effects of an Inclined Magnetic Field on the Unsteady Squeezing Flow between Parallel Plates with Suction/Injection**" is my own work and has not been submitted previously by me for taking any degree from Capital University of Science and Technology, Islamabad or anywhere else in the country/abroad.

At any time if my statement is found to be incorrect even after my graduation, the University has the right to withdraw my M.Phil Degree.

(Ibrahim Jahangeer)

Registration No: MMT173028

Plagiarism Undertaking

I solemnly declare that research work presented in this thesis titled "**Effects of an Inclined Magnetic Field on the Unsteady Squeezing Flow between Parallel Plates with Suction/Injection**" is solely my research work with no significant contribution from any other person. Small contribution/help wherever taken has been dully acknowledged and that complete thesis has been written by me.

I understand the zero tolerance policy of the HEC and Capital University of Science and Technology towards plagiarism. Therefore, I as an author of the above titled thesis declare that no portion of my thesis has been plagiarized and any material used as reference is properly referred/cited.

I undertake that if I am found guilty of any formal plagiarism in the above titled thesis even after award of M.Phil degree, the University reserves the right to withdraw/revoke my M.Phil degree and that HEC and the University have the right to publish my name on the HEC/University website on which names of students are placed who submitted plagiarized work.

(Ibrahim Jahangeer)

Registration No: MMT173028

Acknowledgements

All the praises and thanks to Almighty Allah; the Lord and the Creator of all creations by whom power and glory of all things are accomplished. I would like to give the credit of this thesis to my supervisor **Dr. Shafqat Hussian**, His leadership and words of encouragement perk up my performance throughout the session. I am grateful for his mentorship. Thank you sir!

I would like to convey special thanks to my family members for their support and guidance. I would also take this opportunity to thanks my friends and students of mathematics department, who helped me and made certain corrections in my research.

(Ibrahim Jahangeer)

Registration No: MMT173028

Abstract

The problem of an unsteady squeezing flow of fluid between two parallel plates under the influence of an inclined magnetic field is considered and analyzed. The inclination angle of the applied magnetic field varies from 0^0 to 90^0. Viscous dissipation, Joule heating and the stretching velocity of the lower plate with suction or injection are also taken into account. The transformed nonlinear governing equations are solved numerically by a fourth order Runge-Kutta scheme coupled with the shooting method. Impact of the squeeze number, the magnetic parameter, the magnetic inclination angle, the lower-plate stretching parameter, the lower-plate suction/injection parameter and Eckert number on the velocity and temperature are discussed, respectively. It is found that the inclination angle of the applied magnetic field also plays an important role in the velocity and heat transfer in squeezing flows. The influence of increasing the strength of the magnetic field on velocity and temperature can also be obtained approximately by varying the angle of inclination of the magnetic field used.

Contents

List of Figures

Abbreviations

BVPs	Boundary Value Problems
IVPs	Initial Value Problems
MHD	Magnetohydrodynamics
ODEs	Ordinary Differential Equations
PDEs	Partial Differential Equations
RK	Runge-Kutta

Symbols

(u, v)	velocity components
(x, y)	cartesian coordinates
C_p	specific heat constant $(Jkg^{-1}K^{-1})$
g	gravitational acceleration (m/s^2)
k	thermal conductivity $(Wm^{-1}K^{-1})$
R	lower plate stretching parameter
S_b	lower plate suction/injection parameter
Rd	thermal Radiation perameter
k^*	mean absorption coefficient
η^*	fluid property
u_s	velocity of lower plate
v_H	velocity of upper plate
v_c	lower plate mass flux velocity
Nu	Nusselt number
p	dimensional pressure
P	non-dimensional pressure
q_x	radiative heat flux along $x-$direction (W/m^2)
q_y	radiative heat flux along $y-$direction (W/m^2)
Pr	Prandtl number $(\frac{\nu_f}{\alpha_f})$
Da	Darcy number
Ec	Eckert number
S	Squeeze number
M	Magnetic Number

B_0	magnetic field
T_∞	free stream temperature of nanofluid
γ	Magnetic inclination angle
T_H	temperature of upper plate surface
T_0	temperature of lower plate surface
Re_x	local Reynolds number
Ra	Rayleigh number
Greek symbols	
α	thermal diffusivity (m^2s^{-1})
β	thermal expansion coefficient (K^{-1})
ϕ	volume fraction of nanoparticles
θ	non-dimensional temperature $\left(\frac{T-T_0}{T_H-T_0}\right)$
ρ	nanofluid density (kgm^{-3})
σ	electrical conductivity
μ	dynamic viscosity $(kgm^{-1}s^{-1})$
ν	kinematic viscosity (m^2s^{-1})
σ^*	Stefan-Boltzman constant (KW/m^2k^4)

Chapter 1

Introduction

A substance in the gas or liquid phase is called the fluid. Fluid flow has various aspects, for example, steady and unsteady, compressible and incompressible, viscous and inviscid, rotational and irrotational, uniform and non-uniform etc, Meir [1]. Viscous fluid between parallel plates generates a squeezing movement. The squeezing movement has multiple industrial applications, such as food preservation, injecting design, compression, squeezed films, cooling liquid etc, Stefan [2]. Analysis of the momentum equation is very crucial in such applications and processes of fluid flow. He provided the basic and pioneering research on squeezing movement under lubricating oil assumption. His admirable work opened new doors to explore the squeezing flow. The earlier squeezing movement studies were based on Reynolds equation which was shown by Jackson [3] and Usha and Sridharan [4] to be insufficient for some cases. In a previous research over the several decades, Reynolds [5] studied the squeezing movement between elliptic plates while Archibald [6] examined rectangular plates with the same problem. Mahmood et al. [7] described the squeezed flow analysis for heat transfer on a porous surface. Hayat et al. [8] investigated the affect of chemical response and thermally conductive conditions on squeezing movement. The squeezing effect of combined mass and heat transfer behavior of a viscous fluid flow between parallel plates was demonstrated by Mustafa et al. [9]. Ahmad et al. [10] recently analyzed the

impact of velocity, thermal and solutal slips effects on squeezed fluid transport features. Hayat and Hina [11] discussed the affect on Williamson fluid flow through mass and heat transfer with flexible walls. Farooq et al. [12] also investigated the combined properties of convection of Sutterby fluid squeezing flow in squeezed tube. Consequently some other researchers studied the thermodynamic effects of squeezed flow such as Khaled and Vafai [13] discussed the effect of heat transfer for the squeezed flow of viscous fluid on a sensor surface. Ganji et al. [14] discussed the analytical solution of squeezed flow with magnetic effects between two porous plates and compared the results of suction and blowing cases using the Homotopy fluctuation method. Islam et al. [15] investigated steady axisymmetric squeezing fluid flow in a porous channel. Abd-El Aziz [16] considered an unsteady stretching sheet to be the result of time-dependent chemical process of a viscous fluid flow. Jackson [3] considered and analyzed a theoretical analysis, using an iterative method of squeezing Newtonian liquid flow produced by the unsteady movement of a disk over a plane surface. Acharya et al. [17] investigated the squeezing movement of Cu-water and Cu-kerosene nanofluids flow between two parallel plates. Heat and mass transfer aspects of squeezing a micropolar fluid within a porous medium were examined by Fakour et al. [18] using the least square method. From their analysis it is observed that with the rising values of Reynolds number, the thickness of the velocity boundary layer decreases. Due to the normal movement of the plates, Siddiqui et al. [19] discussed the role of magnetic field in the squeezing movement between parallel plates. The porous medium is the material which consists pores filled by fluid. The potential to allow fluids to pass through porous surface is defined as permeability represented by k. Darcy 's law presented by Henry Darcy denotes the flow through porous medium (1803 – 1858). The purpose of this law is the flowing of water through the beds and sands. The assumptions in the porous medium have become more attractive when Darcy law began to be modified [20].

To maintain flow and heat transfer under the application of magnetic fields has important significance for multiple areas of physics, especially nuclear reactors with MHD generators, geothermal extractions, plasma studies, aeronautical and

aerodynamic boundary layer control, etc. [21–35]. Ansari et al. [36] described the affects of a magnetic field on an irregular hydromagnetic squeezing movement between two parallel plates of an unsteady viscous fluid. Domairry and Aziz [37] studied the squeezing movement between parallel disks under the influence of a magnetic field. Haq et al. [38] investigated the squeezed movement of nanofluid over a sensor surface using MHD. Hayat et al. [39] used the homotopy analysis to investigatedthe impacts of a magnetic field on the squeezing movement of couple stress nanofluid flow between two parallel plates. In the presence of thermal radiation and diffusion, Olajuwon et al. [40] performs the study of heat and mass transfer analysis of second grade MHD fluid. Nadeem et al. [41] explained the impact of Casson MHD fluid flow past linear stretching sheet in a transverse direction. Hatami et al. [42] explained the effect of magnetic field on the study of nanofluid heat transfer between parallel plates. Within a rectangular cavity Rashad et al. [43] examined the free heat transfer flow in the influence of a uniform inclined magnetic field. Kirubhashankar and Ganesh [44] examined an unsteadyMHD flow of a Casson fluid in a parallel plate with a chemical reaction and concluded that an increase in the heat source and Prandtl number reduces the temperature profiles. The heat and mass transfer properties of gyrotactic microorganisms suspended in the MHD Casson fluid flow across a vertical rotating plate or cone maintained in a porous medium were investigated numerically by Raju and Sandeep [45]. Recently, the impacts of a magnetic field on the squeezing movement of an unsteady viscous fluid between parallel plates with suction/injection was analyzed by Su and Yin [46].

The work on the squeezing movement under inclined magnetic fields requires further analysis according to the survey of relevant studies we have found. The present study focused on the flow and convection features of the fluid squeezed among two parallel plates while the magnetic field is inclined by taking inspiration from the above mentioned studies. The surface of the lower plate with suction stretches across the longitudinal direction in the squeezing flow. The resulting governing equations are numerically solved, the impact of the squeeze parameter, the magnetic field parameter, the lower plate stretching parameter, the Darcy number, the

parameter for lower plate suction/injection, the thermal radiation and the Eckert number on the velocity and temperature profile.

1.1 Thesis Contribution

In this thesis, a review study of Su and Yin [46] has been presented and then the flow analysis has been extended in a porous medium. The governing system of nonlinear PDEs is converted into a model of nonlinear ODEs by using appropriate transformation of similarities. Numerical results are obtained for the set of nonlinear ODEs by using the shooting technique with Runge-Kutta method of order four (RK4). The influence of various relevant physical parameters has been discussed using graphs.

1.2 Thesis Outline

This research work is further classified into four main chapters.

Chapter 2 contains some basic definitions, terminologies and governing equations of the fluid which are needed for the upcoming chapters.
Chapter 3 contains the review work of Su and Yin [46]. By utilizing similarity transformation we reduce the set of nonlinear PDEs into a set of nonlinear ODEs and then solve numerically. Numerical results are obtained for the set of nonlinear ODEs with the help of shooting technique.
Chapter 4 extends the work of Su and Yin [46] by considering in a porous medium. The transformation of similarities has been utilized for the conversion of PDEs to ODEs. The transformed nonlinear ODEs are then solved by using the shooting technique that is most common.
Chapter 5 summarizes the research work and gives the main conclusion arising from the whole study.
All the references used in this thesis are presented in Bibliography.

Chapter 2

Fundamental Concepts

In the current chapter we discuss the definitions, basic laws and basic concept related to the fluid dynamics and dimensionless parameters, which will be used in the upcoming chapters. Moreover, the shooting method is also discussed at the end of this chapter.

2.1 Some Basic Definitions

2.1.1 Fluid[47]

"Fluids are substances whose molecular structure offers no resistance to external shear forces: even the smallest force causes deformation of fluid particles. Although a significant distinction exists between liquids and gases, both types of fluids obey the same laws of motion."

2.1.2 Fluid Mechanics[48]

"Fluid mechanics is defined as the science that deals with the behavior of fluids at rest (fluid statics) or in the motion (fluid dynamics), and the interaction of fluids with solids or other fluids at the boundaries."

2.1.3 Fluid Dynamics[49]

"It is the study of the motion of liquids, gases and plasma from one place to another. Fluid dynamics has a wide range of applications like calculating force and moments on aircraft, mass flow rate of petroleum passing through pipelines, prediction of weather, etc."

2.1.4 Fluid Statics[49]

"Fluid statics is the branch of fluid mechanics which studies the fluid at rest and also embraces the characteristics of fluid under the condition of rest means statics condition is known as fluid statics."

2.1.5 Viscosity[50]

"Viscosity is a quantitative measure of a fluids resistance to flow. More specifically, it determines the fluid strain rate that is generated by a given applied shear stress. We can easily move through air, which has very low viscosity.

$$\mu = \frac{\tau}{\frac{\partial u}{\partial y}},$$

where μ is viscosity coefficient, τ is the shear stress and $\frac{\partial u}{\partial y}$ represent the velocity gradient or rate of shear strain. Therefore μ has dimension of stress-time:$\frac{M}{LT}$."

2.1.6 Kinematic Viscosity[51]

"It is defined as the ratio between the dynamic viscosity and density of fluid. It is denoted by the Greek symbol ν, thus mathematically,

$$\nu = \frac{\mu}{\rho},$$

where the dimension of kinematic viscosity is $\frac{L^2}{T}$."

2.2 Classification of Fluids

2.2.1 Ideal Fluid[51]

"A fluid which is incompressible and is having no viscosity($\mu = 0$), is known as an ideal fluid. An ideal fluid is only an imaginary fluid as all the fluids, which exist have some viscosity."

2.2.2 Real Fluid[51]

"A fluid which possesses viscosity is known as real or viscous fluid having($\mu > 0$). All the fluids, in actual practice, are real fluids."

2.2.3 Newtonian Fluid[51]

"A real fluid, in which shear stress is directly proportional to the rate of shear strain (or velocity gradient) is known as a Newtonian fluid. Mathematically defined as

$$\tau = \mu \frac{\partial u}{\partial y},$$

where τ is the shear stress, u denotes the x-component of velocity and ν denotes dynamic viscosity. The common examples of Newtonian fluids are air, oxygen gas, alcohol, milk, glycerol and silicone/thin motor oil etc."

2.2.4 Non-Newtonian Fluid[51]

"A real fluid in which the shear stress is not proportional to the rate of shear strain (or velocity gradient), is known as a non-Newtonian fluid. Mathematically, it can be expressed as

$$\tau_{xy} \propto \left(\frac{du}{dy}\right)^m, m \neq 1.$$

$$\tau_{xy} = \nu \left(\frac{du}{dy} \right), \quad v = j \left(\frac{du}{dy} \right)^{m-1}$$

where ν denotes the apparent viscosity, m is the index of flow performance and the constancy index is j. Note that for m= 1, above equation reduces to the Newton's law of viscosity. Examples of non-Newtonian fluids are toothpaste, ketchup, starch suspensions, custard, shampoo, paint and blood etc."

2.2.5 Ideal Plastic Fluid[51]

"A real fluid, in which shear stress is more than the yield value and shear stress is proportional to the rate of shear strain (or velocity gradient), is known as an ideal plastic fluid."

2.3 Heat Transfer Mechanism and Related Properties

2.3.1 Conduction[52]

"Due to collision of molecules in the contact form, heat is transferred from one object to another object this phenomenon is called conduction.

$$Q = -kA \left(\frac{\Delta T}{\Delta n} \right),$$

where k denotes the constant of the thermal conductivity and $\frac{\Delta T}{\Delta n}$ denotes gradient of temperature respectively."

2.3.2 Heat Transfer[52]

"Due to temperature difference, energy transfer is called heat transfer. Heat transfer occurs through different mechanisms."

2.3.3 Radiation[52]

"In the radiation process, heat is transferred through electromagnetic rays and waves. It takes place in liquids and gasses. An example of radiation would be atmosphere, the atmosphere is heated by the radiation of the sun."

2.3.4 Thermal Conductivity[52]

"It is the property of a substance which measures the ability to transfer heat. Fourier's law of conduction which relates the flow rate of heat by conduction to the temperature gradient is

$$\frac{dQ}{dt} = -kA\frac{dT}{dx},$$

where A, k, $\frac{dQ}{dt}$ and $\frac{dT}{dx}$ are the area, the thermal conductivity, the temperature and the rate of heat transfer, respectively. The SI unit of thermal conductivity is $\frac{kgm}{s^3}$ and the dimension of thermal conductivity is $\left[\frac{ML}{T^3}\right]$."

2.3.5 Thermal Diffusivity[52]

"The ratio of the unsteady heat conduction k of a substance to the product of specific heat capacity C_p and density ρ is called thermal dffusivity.

$$\alpha = \frac{k}{\rho C_p},$$

The unit and dimension of thermal Diffusivity in SI system are m^2/s and $[LT^{-1}]$ respectively."

2.3.6 Convection[52]

"The process in which fluid is forced by external processes and when thermal energy expands in gravitational fields by the interaction of buoyancy forces then

it is called convection. Gases and liquid are the examples of convection fluid. Mathematically, it is expressed as

$$q = hA(T_s - T_\infty),$$

where h, A, T_s and T_∞ expresses the heat transfer coefficient, the area, the temperature of the surface. It is further simplified into following three categories."

2.4 Types of Flow

2.4.1 Compressible flow[48]

"A compressible flow is the branch of fluid mechanics which varies significant changes during the fluid flow used in high-speed jet engines, aircraft, rocket motors also in high-speed usage in a planetary atmosphere, gas pipelines and in commercial fields." Mathematically, it is expressed as

$$\rho(x, y, z, t) \neq c,$$

2.4.2 Incompressible flow[48]

"A type of fluid flow mechanics in which the density remains constant throughout during the flow, is called incompressible flow." Mathematically, it is expressed as

$$\rho(x, y, z, t) = c,$$

2.4.3 Laminar flow[48]

"In fluid dynamics, laminar flow occurs when a flow is in parallel layers/closed channel or at plates with no interruption between the plates. Typically, each

particle has a definite path and the particles of the path in the fluid do not cross each other. Rising of smoke is an example of laminar flow."

2.4.4 Turbulent flow[48]

"When fluid undergoes irregular fluctuations or flowing faster, this type of fluid (liquid or gas) is called turbulent flow. Turbulent flow which moves randomly in any direction and has no definite path and can't be handled easily. It undergoes changes both in magnitude and direction."

2.4.5 Steady flow[48]

"The flow that does not changes with respect to time is called steady flow. Mathematically, it can be written as

$$\frac{d\eta^*}{dt} = 0,$$

where η^* is fluid property."

2.4.6 Unsteady flow[48]

"The flow that continuously changes with respect to time, is expressed as unsteady flow." Mathematically, it can be written as

$$\frac{d\eta^*}{dt} \neq 0,$$

2.4.7 Uniform flow[48]

"The flow defined in which velocity and hydrodynamic parameters does not changes from point to point at any given instant, having same direction as well as magnitude during the fluid motion called as uniform flow. Mathematically, it can be

expressed as

$$\frac{\partial \mathrm{V}}{\partial s} = 0,$$

where V is the velocity and s is the displacement."

2.4.8 Non-uniform flow[48]

"In non-uniform flow, the velocity and hydrodynamic parameters changes from one point to another point and the velocity is not same at every point of the fluid at an instant. Mathematically, it is written as

$$\frac{\partial \mathrm{V}}{\partial s} \neq 0,$$

where V is the velocity and s is the displacement in direction."

2.5 Fundamental Equations of Flow

2.5.1 Continuity Equation[53]

"The conservation of mass of fluid entering and leaving the control volume, the resulting mass balance is called the equation of continuity. This equation reflects the fact that mass is conserved.

Mathematically it can be write as

$$\frac{\partial \rho}{\partial t} + \nabla.\ (\rho \mathrm{V}) = 0. \tag{2.1}$$

For steady case rate of time will be constant, so continuity equation becomes

$$\nabla.\ (\rho \mathrm{V}) = 0. \tag{2.2}$$

In the case of incompressible flow, density does not variate so continuity equation can be re-write as,

$$\nabla .\ \mathrm{V} = 0. \tag{2.3}$$

Where, V is velocity of fluid."

2.5.2 Equation of Momentum[53]

"For any fluid the momentum equation is

$$\frac{\partial}{\partial t}(\rho \mathrm{V}) + \nabla .[(\rho \mathrm{V})\mathrm{V}] - \nabla .\mathrm{T} - \rho \mathbf{g} = 0. \tag{2.4}$$

Since $\mathrm{T} = -p\mathrm{I} + \tau$, the momentum equation takes the form

$$\rho \left(\frac{\partial \mathrm{V}}{\partial t} + \mathrm{V}.\nabla \mathrm{V} \right) = \nabla .(-p\mathrm{I} + \tau) + \rho \mathbf{g}. \tag{2.5}$$

Equation (2.4) is a vector equation and can be decomposed further into three scalar components by taking the scalar product with the basis vectors of an appropriate orthogonal coordinate system. By setting $\mathbf{g} = g\nabla z$, where z is the distance from an arbitrary reference elevation in the direction of gravity, Equation (2.4) can also be expressed as

$$\rho \frac{D\mathrm{V}}{Dt} = \rho \left(\frac{\partial \mathrm{V}}{\partial t} + \mathrm{V}.\nabla \mathrm{V} \right) = \nabla .(-p\mathrm{I} + \tau) + \rho (g \nabla z). \tag{2.6}$$

Where $\frac{D}{Dt}$ is the substantial derivative. The momentum equation then states that the acceleration of a particle following the motion is the result of a net force, expressed by the gradient of pressure, viscous and gravity forces."

2.5.3 Law of Conservation of Energy[53]

"Conservation of thermal energy is expressed by

$$\rho \left[\frac{\partial U}{\partial t} + \mathrm{V}.\nabla U \right] = [\tau : \nabla \mathrm{V} + p \nabla .\mathrm{V}] + \nabla (k \nabla \mathrm{T}) \pm H_r, \tag{2.7}$$

where U is the internal energy per unit mass, and H_r is the heat of reaction. By involving the definition of the internal energy,

$$\rho C_v \left[\frac{\partial \mathrm{T}}{\partial t} + \mathrm{V}.\nabla \mathrm{T}\right] = [\tau : \nabla \mathrm{V} + p\nabla.\mathrm{V}] + \nabla(k\nabla \mathrm{T}) \pm H_r. \tag{2.8}$$

For heat conduction in solids, i.e, when $\mathrm{V} = 0$, $\nabla \mathrm{V} = 0$ and $C_v = C$, the resulting equation is

$$\rho C \frac{\partial \mathrm{T}}{\partial t} = \nabla(k\nabla t) \pm H_r." \tag{2.9}$$

2.6 Dimensionless Parameters

2.6.1 Reynolds Number(Re)[52]

"It is the ratio of the inertial forces to the viscous forces. Based on their behavior, the fluid flows are identified as laminar or turbulent flow. Mathematically, it is expressed as

$$\begin{aligned} R_e &= \frac{\rho U^2}{L}\frac{L^2}{\mu U}, \\ R_e &= \frac{LU}{\nu}, \end{aligned} \tag{2.10}$$

where U denotes the free stream velocity, L is the characteristics length and ν stands for kinematic viscosity."

2.6.2 Prandtl Number(Pr)[53]

"The ratio of kinematic diffusivity to heat the diffusivity is said to be Prandtl number. It is denoted by Pr Mathematically, it can be written as

$$\begin{aligned} P_r &= \frac{\nu}{\alpha}, \\ P_r &= \frac{\mu c_p}{\rho k}, \end{aligned} \tag{2.11}$$

where μ and α denote the momentum diffusivity or kinetic diffusivity and thermal diffusivity respectively. Here c_p denotes the specific heat and k stands for thermal conductivity."

2.6.3 Nusselt Number(Nu)[52]

"It is the relationship between the convective to the conductive heat transfer through the boundary of the surface. It is a dimensionless number which was first introduced by the German mathematician Nusselt.
Mathematically, it is defined as:

$$Nu = \frac{hL}{k}, \tag{2.12}$$

where h stands for convective heat transfer, L stands for characteristics length and stands for thermal conductivity."

2.6.4 Darcy Number(Da)[52]

"The Darcy number Da represents the effect of the permeability of medium according to its cross sectional area.

$$Da = \frac{k}{H^2}, \tag{2.13}$$

where k shows the permeability of porus medium and H is the length of prescribed geometry. It was first introduced by Henry Darcy. It is transformed by the non dimensionalizing the differential form of Darcy's law."

2.6.5 Skin Friction Coefficient(C_f)[54]

"The skin friction coefficient is typically defined as

$$C_f = \frac{2\tau_w}{\rho w_\infty^2}, \tag{2.14}$$

where τ_w is the local wall shear stress, ρ is the fluid density and w_∞ is the free stream velocity (usually taken outside the boundary layer or at the inlet). It expresses the dynamic friction resistance originating in viscous fluid flow around a fixed wall."

2.6.6 Eckert Number(Ec)[54]

"A number with no dimensions used in continuum mechanics. It defines the "relationship between flow's kinetic energy and boundary layer difference."
Mathematically it can be written as,

$$Ec = \frac{\mathrm{V}^2}{C_p R^2 (T_H - T_0)},\text{"} \tag{2.15}$$

"where V is the velocity of the fluid, R is the lower-plate stretching parameter, C_p is the specfic heat and δT is the original and final temperature variations."

2.6.7 Rayleigh Number(Ra)[54]

"It is the relationship between the kinematic diffusivity to heat diffusivity multiplied by the ratio of viscosity forces and buoyancy forces.It is a dimensionless number introduced by Lord Rayleigh.

It is denoted by Ra and mathematically it can be written as

$$Ra = \frac{g\beta}{\nu\alpha}(T_h - T_c)L^3.\text{"} \tag{2.16}$$

2.7 Solution Methodology

"Consider the second order two point boundary value problem (BVP):

$$u'' = f(x, u, u') \tag{2.17}$$

subjected to the boundary conditions:

$$u(0) = 0 \quad , \quad u(\alpha) = \xi,$$

where ξ is some known constant. In order to apply the shooting method for the BVP (2.17), we first convert the equation (2.17) into a system of two first order ODEs. Using the notation, $u = u_1, \quad u' = u_1' = u_2, \;\; u'' = u_1'' = u_2'$ we have

$$u_1' = u_2, \tag{2.18}$$

$$u_2' = f(x, u_1, u_2). \tag{2.19}$$

The associated boundary conditions reduced as:

$$u_1(0) = 0 \quad , \quad u_1(\alpha) = \xi.$$

By considering $u_2(0) = \eta$, the first order system of Eqs. (2.18) and (2.19) together with $u_1(0) = 0$, $u_2(0) = \eta$ is an initial value problem (IVP) and can be solved by using the Runge-Kutta method of order four (RK4). Then we get both u_1 and u_2 computed at the decided nodes. If $u_1(\alpha)$ is sufficiently close to ξ, then this u_1 is an approximate solution, if not we have to choose another value of ξ and the process is repeated again. Newton method is used to refine the initial guess. This process is continued until a satisfactory accuracy is achieved. Its main advantage is its efficiency and fastness. If the solution is extremely sensitive to the assumed initial condition, then parallel shooting method is applied (see Na [55] for details)."

Chapter 3

Effects of a Magnetic Field on Unsteady Squeezing Flow of Viscous Fluid

The problem of an unsteady squeezing movement of fluid between two parallel plates are studied under the impact of magnetic field. As the plates move closer to each other, squeezing movement is perpendicular to the surfaces of the plates. The governing system of nonlinear PDEs is converted into a model of nonlinear ODEs by utilizing the transformation of similarities. Apart from it the solution of ODEs has been acquired by using the shooting technique. At the end of chapter the numerical solutions of ODEs have been discussed with impact on the skin friction coefficients, Nusselt number, velocity and temperature. The data is represented and analyzed with the help of graphs. In this chapter, the review work of Su and Yin [46] is presented.

3.1 Mathematical Modeling

We considered the problem of the unsteady squeezing movement of a viscous fluid bounded between two infinite parallel plates that are subject to magnetic field **B**

as shown in Figure 3.1. The channel's lower plate is along x-axis and the y-axis normal to it. The time-dependent magnetic field $\mathbf{B} = (B_m \cos\gamma, B_m \sin\gamma, 0)$, in which B_m denotes $B_0(1-\alpha t)^{-1/2}$, is applied along the magnetic inclination angle γ. For a small magnetic Reynolds number the induced magnetic field is assumed to be negligible. With respect to time t, the distance between the plates $H(t) = l(1-\alpha t)^{1/2}$ change, where the initial distance between the plates is l at $t = 0$. When $\alpha < 0$ as the plates move apart and for $\alpha > 0$, the two plates are squeezed, u_s is the velocity of the lower plate, v_H is the velocity of the upper plates, v_c is the lower plate mass flux velocity, T_H is the upper plate surface temperature, T_0 denotes the lower plate surface temperature.

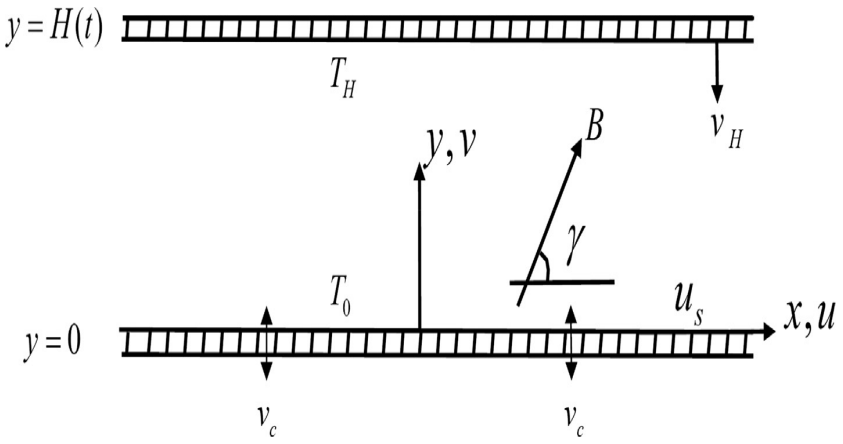

Figure 3.1: Geometry of the Physical Model.

The governing PDEs are:

$$\frac{\partial u}{\partial x} + \frac{\partial v}{\partial y} = 0, \tag{3.1}$$

$$\frac{\partial u}{\partial t} + u\frac{\partial u}{\partial x} + v\frac{\partial u}{\partial y} = -\frac{1}{\rho}\frac{\partial p}{\partial x} + \frac{\mu}{\rho}\left(\frac{\partial^2 u}{\partial x^2} + \frac{\partial^2 u}{\partial y^2}\right) + \frac{\sigma B_m^2}{\rho}\sin\gamma(v\cos\gamma - u\sin\gamma), \tag{3.2}$$

$$\frac{\partial v}{\partial t} + u\frac{\partial v}{\partial x} + v\frac{\partial v}{\partial y} = -\frac{1}{\rho}\frac{\partial p}{\partial y} + \frac{\mu}{\rho}\left(\frac{\partial^2 v}{\partial x^2} + \frac{\partial^2 v}{\partial y^2}\right) + \frac{\sigma B_m^2}{\rho}\cos\gamma(u\sin\gamma - v\cos\gamma), \tag{3.3}$$

$$\frac{\partial T}{\partial t} + u\frac{\partial T}{\partial x} + v\frac{\partial T}{\partial y} = \frac{k}{\rho c_p}\left(\frac{\partial^2 T}{\partial x^2} + \frac{\partial^2 T}{\partial y^2}\right) + \frac{\mu}{\rho c_p}\left[2\left(\frac{\partial u}{\partial x}\right)^2 + 2\left(\frac{\partial v}{\partial y}\right)^2 + \left(\frac{\partial u}{\partial y} + \frac{\partial v}{\partial x}\right)^2\right] + \frac{\sigma B_m^2}{\rho c_p}(u\sin\gamma - v\cos\gamma)^2. \tag{3.4}$$

3.1.1 Dimensional Boundary Conditions

The dimensional form of the BCs is:

$$u = u_s = \frac{bx}{1-\alpha t}, \quad v = v_c = -\frac{v_0}{\sqrt{1-\alpha t}}, \quad T = T_0 \quad \text{at} \quad y = 0, \tag{3.5}$$

$$u = 0, v = v_H = \frac{dH}{dt} = -\frac{\alpha l}{2\sqrt{1-\alpha t}}, \quad T = T_H = T_0 + \frac{T_0}{1-\alpha t} \text{ at } y = H(t). \tag{3.6}$$

To transform the modeled equations (3.1)-(3.4) into the dimensionless form, these are the similarity transformation that defined in [46] has been used:

$$\eta = \frac{y}{l(1-\alpha t)^{1/2}}, \quad v = v_H f(\eta), \quad u = -\frac{x v_H f'(\eta)}{l(1-\alpha t)^{1/2}}, \quad \theta(\eta) = \frac{T - T_0}{T_H - T_0}. \tag{3.7}$$

By using (3.7) into (3.1), the continuity equation is satisfied. Take u and differentiating w.r.t 'x',

$$\begin{aligned} u &= -\frac{x v_H f'(\eta)}{H(t)}, \\ \frac{\partial u}{\partial x} &= \frac{\partial}{\partial x}\left(\frac{-x v_H f'(\eta)}{H(t)}\right), \\ \frac{\partial u}{\partial x} &= -\frac{v_H f'(\eta)}{H(t)}. \end{aligned} \tag{3.8}$$

Similarly differentiating v w.r.t 'y',

$$\begin{aligned} v &= v_H f(\eta), \\ \frac{\partial v}{\partial y} &= \frac{\partial}{\partial y}\left(v_H f(\eta)\right), \\ &= v_H\ f'(\eta)\ \eta'(y), \\ \frac{\partial v}{\partial y} &= \frac{v_H\ f'(\eta)}{H(t)}. \end{aligned} \tag{3.9}$$

Using (3.8)-(**??**) in (3.1) to satisfy continuity equation

$$\frac{\partial u}{\partial x}+\frac{\partial v}{\partial y}=-\frac{v_H f'(\eta)}{H(t)}+\frac{v_H f'(\eta)}{H(t)}=0. \tag{3.10}$$

Now we include the procedure for the conversion of (3.2) and (3.3) into dimensionless form.

Converting PDEs of momentum equations into ODE to utilize transformation of similarities, so differentiating (3.2) w.r.t 'y' and (3.3) w.r.t 'x' and subtracting to eliminate the pressure gradient we proceed as follows.

$$\begin{aligned}&\frac{\partial}{\partial y}\left(\frac{\partial u}{\partial t}+u\frac{\partial u}{\partial x}+v\frac{\partial u}{\partial y}\right)-\frac{\partial}{\partial x}\left(\frac{\partial v}{\partial t}+u\frac{\partial v}{\partial x}+v\frac{\partial v}{\partial y}\right)=-\frac{1}{\rho}\frac{\partial^2 p}{\partial y\partial x}\\&+\frac{1}{\rho}\frac{\partial^2 p}{\partial x\partial y}+\nu\frac{\partial}{\partial y}\left(\frac{\partial^2 u}{\partial x^2}+\frac{\partial^2 u}{\partial y^2}\right)-\nu\frac{\partial}{\partial x}\left(\frac{\partial^2 v}{\partial x^2}+\frac{\partial^2 v}{\partial y^2}\right)\\&+\frac{\sigma B_m^2}{\rho}\left[\sin\gamma\frac{\partial}{\partial y}(v\cos\gamma-u\sin\gamma)-\cos\gamma\frac{\partial}{\partial x}(u\sin\gamma-v\cos\gamma)\right].\end{aligned} \tag{3.11}$$

'v' does not depend on x so the derivative of v is zero and second derivative of u is also zero.

$$\begin{aligned}v=v_H f(\eta)\quad;\quad u=-\frac{xv_H f'(\eta)}{H(t)},\\\frac{\partial v}{\partial x}=0\quad;\quad\frac{\partial^2 u}{\partial x^2}=0.\end{aligned}$$

So we have,

$$\begin{aligned}\frac{\partial}{\partial y}\left(\frac{\partial u}{\partial t}+u\frac{\partial u}{\partial x}+v\frac{\partial u}{\partial y}\right)=\nu\frac{\partial^3 u}{\partial y^3}+\frac{\sigma B_m^2}{\rho}\sin\gamma\cos\gamma\frac{\partial v}{\partial y}-\frac{\sigma B_m^2}{\rho}\sin^2\gamma\frac{\partial u}{\partial y}\\-\frac{\sigma B_m^2}{\rho}\sin\gamma\cos\gamma\frac{\partial u}{\partial x},\end{aligned}$$

$$\begin{aligned}\frac{\partial^2 u}{\partial y\partial t}+u\frac{\partial^2 u}{\partial y\partial x}+v\frac{\partial^2 u}{\partial y^2}=\nu\frac{\partial^3 u}{\partial y^3}+\frac{\sigma B_m^2}{\rho}\sin\gamma\cos\gamma\frac{\partial v}{\partial y}-\frac{\sigma B_m^2}{\rho}\sin^2\gamma\frac{\partial u}{\partial y}\\-\frac{\sigma B_m^2}{\rho}\sin\gamma\cos\gamma\frac{\partial u}{\partial x}.\end{aligned} \tag{3.12}$$

Take η and differentiating w.r.t 't',

$$\begin{aligned}\frac{\partial \eta}{\partial t} &= \frac{\partial}{\partial t}\left(\frac{y}{l\ (1-\alpha t)^{\ 1/2}}\right),\\ \frac{\partial \eta}{\partial t} &= \frac{\alpha y}{2l(1-\alpha t)^{3/2}}.\end{aligned} \tag{3.13}$$

The derived form of u by using v_H becomes

$$\begin{aligned}u &= \frac{-xv_H f'(\eta)}{l(1-\alpha t)^{1/2}} \quad ; \quad v_H = \frac{-\alpha l}{2\sqrt{1-\alpha t}}\\ u &= \frac{\frac{x\alpha l f'(\eta)}{2\sqrt{1-\alpha t}}}{l(1-\alpha t)^{1/2}},\\ u &= \frac{\alpha x f'(\eta)}{2(1-\alpha t)}.\end{aligned}$$

Take u and differentiating w.r.t 't',

$$\begin{aligned}u &= \frac{\alpha x f'(\eta)}{2(1-\alpha t)},\\ \frac{\partial u}{\partial t} &= \frac{\partial}{\partial t}\left(\frac{\alpha x f'}{2(1-\alpha t)}\right),\\ &= \frac{\alpha x f''}{2(1-\alpha t)}\frac{\partial}{\partial t}\left(\frac{y}{l\ (1-\alpha t)^{\ 1/2}}\right) + \frac{\alpha\ x\ f'}{2}\ \frac{\partial}{\partial t}\ \left(\frac{1}{1-\alpha t}\right),\\ &= \frac{\alpha^2 xyf''}{4l(1-\alpha t)^{5/2}} + \frac{\alpha^2 x f'}{2(1-\alpha t)^2}.\end{aligned} \tag{3.14}$$

Again differentiating w.r.t 'y',

$$\begin{aligned}\frac{\partial}{\partial y}\left(\frac{\partial u}{\partial t}\right) &= \frac{\partial}{\partial y}\left(\frac{\alpha^2 xyf''}{4l(1-\alpha t)^{5/2}}\right) + \frac{\partial}{\partial y}\left(\frac{\alpha^2 x f'}{2(1-\alpha t)^2}\right),\\ \frac{\partial^2 u}{\partial y \partial t} &= \frac{\alpha^2 x f''}{4l(1-\alpha t)^{5/2}} + \frac{\alpha^2 xyf'''}{4l(1-\alpha t)^{5/2}}\frac{\partial}{\partial y}\left(\frac{y}{l(1-\alpha t)^{1/2}}\right)\\ &\qquad + \frac{\alpha^2 x f''}{2(1-\alpha t)^2}\frac{\partial}{\partial y}\left(\frac{y}{l(1-\alpha t)^{1/2}}\right),\\ &= \frac{\alpha^2 x f''}{4l(1-\alpha t)^{5/2}} + \frac{\alpha^2 xyf'''}{4l^2(1-\alpha t)^3} + \frac{\alpha^2 x f''}{2l(1-\alpha t)^{5/2}},\\ &= \frac{\alpha^2 xyf'''}{4l^2(1-\alpha t)^3} + \frac{3\alpha^2 x f''}{4l(1-\alpha t)^{5/2}}.\end{aligned} \tag{3.15}$$

Take u and differentiating w.r.t 'x',

$$\begin{aligned} u &= \frac{\alpha x f'(\eta)}{2(1-\alpha t)}, \\ \frac{\partial u}{\partial x} &= \frac{\partial}{\partial x}\left(\frac{\alpha x\ f'}{2\ (1-\alpha t)}\right), \\ \frac{\partial u}{\partial x} &= \frac{\alpha f'}{2\ (1-\alpha t)}. \end{aligned} \tag{3.16}$$

Again differentiating w.r.t 'y', we have

$$\begin{aligned} \frac{\partial^2 u}{\partial x \partial y} &= \frac{\alpha f''}{2(1-\alpha t)}\left(\frac{\partial \eta}{\partial y}\right), \\ \frac{\partial^2 u}{\partial x \partial y} &= \frac{\alpha f''}{2(1-\alpha t)}\left(\frac{1}{l(1-\alpha t)^{1/2}}\right), \\ \frac{\partial^2 u}{\partial x \partial y} &= \frac{\alpha f''}{2l(1-\alpha t)^{3/2}}, \\ u\frac{\partial^2 u}{\partial x \partial y} &= \frac{\alpha^2 x f' f''}{4l(1-\alpha t)^{5/2}}. \end{aligned} \tag{3.17}$$

Take u and differentiating w.r.t 'y',

$$\begin{aligned} u &= \frac{\alpha x f'(\eta)}{2(1-\alpha t)}, \\ &= \frac{\partial}{\partial y}\left(\frac{\alpha x f'}{2(1-\alpha t)}\right), \\ &= \frac{\alpha x f''}{2(1-\alpha t)}\frac{\partial}{\partial y}\left(\frac{y}{l\ (1-\alpha\ t)^{\ 1/2}}\right), \\ \frac{\partial u}{\partial y} &= \frac{\alpha x f''}{2\ l\ (1-\alpha\ t)^{\ 3/2}}. \end{aligned} \tag{3.18}$$

Multiply v on both sides of (3.18), we have

$$\begin{aligned} v\ \frac{\partial u}{\partial y} &= \left(\frac{-\alpha l f}{2\ (1-\alpha t)^{\ 1/2}}\right)\left(\frac{\alpha x f''}{2l(1-\alpha t)^{3/2}}\right), \\ &= \frac{-\alpha^2 x f f''}{4(1-\alpha t)^2}. \end{aligned}$$

Again differentiate w.r.t 'y',

$$v\frac{\partial^2 u}{\partial y^2} = \frac{\partial}{\partial y}\left(\frac{-\alpha^2 x f f''}{4(1-\alpha t)^2}\right),$$

$$= \frac{-\alpha^2 x}{4(1-\alpha t)^2}\left(f\frac{\partial f''}{\partial y} + f''\frac{\partial f}{\partial y}\right)$$

$$v\frac{\partial^2 u}{\partial y^2} = \frac{-\alpha^2 x}{4(1-\alpha t)^2}\left(f f'''\eta'(y) + f'' f'\eta'(y)\right)$$

$$\therefore \left(\eta = \frac{y}{H(\ t)} \quad ; \quad H(t) = l\ (1-\alpha\ t)^{\ 1/2}\right)$$

$$v\frac{\partial^2 u}{\partial y^2} = \frac{-\alpha^2 x}{4(1-\alpha t)^2}\left(f f'''\frac{1}{l\ (\ 1-\alpha\ t)^{\ 1/2}} + f''\ f'\ \frac{1}{l\ (1-\alpha\ t)^{\ 1/2}}\right)$$

$$v\frac{\partial^2 u}{\partial y^2} = \frac{-\alpha^2 x}{4l(1-\alpha t)^{5/2}}(f f''' + f' f''). \tag{3.19}$$

The derived form of v by using v_H,

$$v = v_H f(\eta) \quad ; \quad v_H = \frac{-\alpha l}{2\sqrt{1-\alpha t}},$$

$$v = \frac{-\alpha l f(\eta)}{2\sqrt{1-\alpha t}}.$$

Take v and differentiating w.r.t 'y',

$$\frac{\partial v}{\partial y} = \frac{\partial}{\partial y}\left(\frac{-\alpha l f}{2(1-\alpha t)^{1/2}}\right),$$

$$= \frac{-\alpha l f'}{2(1-\alpha t)^{1/2}}\frac{\partial}{\partial y}\left(\frac{y}{l(1-\alpha t)^{1/2}}\right),$$

$$= \frac{-\alpha l f'}{2(1-\alpha t)^{1/2}}\left(\frac{1}{l(1-\alpha t)^{1/2}}\right),$$

$$\frac{\partial v}{\partial y} = \frac{-\alpha f'}{2(1-\alpha t)}. \tag{3.20}$$

Take (3.18) and again differentiating w.r.t 'y',

$$\frac{\partial^2 u}{\partial y^2} = \frac{\partial}{\partial y}\ \left(\frac{\alpha\ x\ f''}{2\ l\ (1-\alpha t)^{\ 3/2}}\right),$$

$$= \frac{\alpha x f'''}{2\ l\ (1-\alpha\ t)^{\ 3/2}}\frac{\partial}{\partial y}\left(\frac{y}{l(1-\alpha t)^{1/2}}\right),$$

$$\frac{\partial^2 u}{\partial y^2} = \frac{\alpha x f'''}{2l^2(1-\alpha t)^2}.$$

Again differentiating w.r.t 'y',

$$\frac{\partial^3 u}{\partial y^3} = \frac{\partial}{\partial y}\left(\frac{\alpha x f'''}{2l^2(1-\alpha t)^2}\right),$$

$$\frac{\partial^3 u}{\partial y^3} = \frac{\alpha x f^{(iv)}}{2l^2(1-\alpha t)^2}\frac{\partial}{\partial y}\left(\frac{y}{l(1-\alpha t)^{1/2}}\right),$$
$$\nu\frac{\partial^3 u}{\partial y^3} = \frac{\alpha\nu x f^{(iv)}}{2l^3(1-\alpha t)^{5/2}}. \tag{3.21}$$

Using (3.15)-(3.21) in (3.12) becomes

$$\frac{\alpha^2 xyf'''}{4l^2(1-\alpha t)^3} + \frac{3\alpha^2 xf''}{4l(1-\alpha t)^{5/2}} + \frac{\alpha^2 xf'f''}{2l(1-\alpha t)^{5/2}} - \frac{\alpha^2 x}{4l(1-\alpha t)^{5/2}}(ff''' + f'f'')$$
$$= \frac{\alpha\nu x f^{(iv)}}{2l^3(1-\alpha t)^{5/2}} - \frac{\sigma B_m^2}{\rho}\sin\gamma\cos\gamma\frac{\alpha f'}{2(1-\alpha t)} - \frac{\sigma B_m^2}{\rho}\sin^2\gamma\frac{\alpha x f''}{2l(1-\alpha t)^{3/2}}$$
$$- \frac{\sigma B_m^2}{\rho}\sin\gamma\cos\gamma\frac{\alpha f'}{2(1-\alpha t)},$$
$$\therefore \left(B_m = B_0(1-\alpha t)^{-1/2}\right),$$

$$\frac{\alpha^2 xyf'''}{4l^2(1-\alpha t)^3} + \frac{3\alpha^2 xf''}{4l(1-\alpha t)^{5/2}} + \frac{\alpha^2 xf'f''}{2l(1-\alpha t)^{5/2}} - \frac{\alpha^2 x}{4l(1-\alpha t)^{5/2}}(ff''' + f'f'')$$
$$= \frac{\alpha\nu x f^{(iv)}}{2l^3(1-\alpha t)^{5/2}} - \frac{\sigma B_0^2(1-\alpha t)^{-1}}{\rho}\sin\gamma\cos\gamma\frac{\alpha f'}{2(1-\alpha t)}$$
$$- \frac{\sigma B_0^2(1-\alpha t)^{-1}}{\rho}\sin^2\gamma\frac{\alpha x f''}{2l(1-\alpha t)^{3/2}} - \frac{\sigma B_0^2(1-\alpha t)^{-1}}{\rho}\sin\gamma\cos\gamma\frac{\alpha f'}{2(1-\alpha t)},$$

$$\frac{\alpha^2 xyf'''}{4\ l^2(1-\alpha t)^3} + \frac{3\alpha^2 xf''}{4\ l\ (1-\alpha\ t)^{\ 5/2}} + \frac{\alpha^2 x\ f'\ f''}{2\ l\ (1-\alpha\ t)^{\ 5/2}} - \frac{\alpha^2 x}{4\ l\ (1-\alpha t)^{5/2}}(ff''' + f'f'')$$
$$= \frac{\alpha\nu x f^{(iv)}}{2l^3(1-\alpha t)^{5/2}} - \frac{\sigma B_0^2}{\rho}\sin\gamma\cos\gamma\frac{\alpha f'}{2(1-\alpha t)^2} - \frac{\sigma B_0^2}{\rho}\sin^2\gamma\frac{\alpha x f''}{2l(1-\alpha t)^{5/2}}$$
$$- \frac{\sigma B_0^2}{\rho}\sin\gamma\cos\gamma\frac{\alpha f'}{2(1-\alpha t)^2}. \tag{3.22}$$

Multiply $\frac{2l^3(1-\alpha t)^{5/2}}{\alpha\nu x}$ on both sides, the dimensionless form of (3.12) can be reduced as:

$$f^{(iv)} + \frac{l^2\alpha}{2\nu}(ff''' - 3f'' - f'f'' - \eta f''') - \frac{\alpha\sigma l^2 B_0^2}{\rho\nu}\sin\gamma(2\delta f'\cos\gamma + f''\sin\gamma) = 0,$$
$$f^{(iv)} + S(ff''' - 3f'' - f'f'' - \eta f''') - M^2\sin\gamma\,(\sin\gamma f'' + 2\delta\cos\gamma f') = 0. \tag{3.23}$$

Now we have to convert PDE of energy equation into ODE to utilize similarity

transformation, in (3.4) T and v does not depend on x so the derivative of T and v is equal to zero,

$$T = \theta(\eta)(T_H - T_0) + T_0,$$
$$v = v_H f(\eta),$$
$$T_H = T_0 + \frac{T_0}{1 - \alpha t}$$

$$\frac{\partial T}{\partial t} + v\frac{\partial T}{\partial y} = \frac{k}{\rho c_p}\frac{\partial^2 T}{\partial y^2} + \frac{\mu}{\rho c_p}\left[2\left(\frac{\partial u}{\partial x}\right)^2 + 2\left(\frac{\partial v}{\partial y}\right)^2 + \left(\frac{\partial u}{\partial y}\right)^2\right] + \frac{\sigma B_m^2}{\rho c_p}(u\sin\gamma - v\cos\gamma)^2. \tag{3.24}$$

Take T and differentiating w.r.t 't',

$$\begin{aligned} T &= \theta(\eta)\left(\frac{T_0}{1-\alpha\, t} + T_0\right), \\ &= \frac{\partial}{\partial t}\left(\theta(\eta)\,\frac{T_0}{(1-\alpha t)} + T_0\right), \\ &= \theta(\eta)\left(\frac{\alpha T_0}{(1-\alpha t)^{\,2}}\right) + \frac{T_0\,\theta'(\eta)}{(1-\alpha t)}\,\frac{\partial \eta}{\partial t}, \\ \frac{\partial T}{\partial t} &= \frac{\theta(\,\eta\,)\,\alpha T_0}{(1-\alpha t)^2} - \frac{\theta'(\eta) T_0 y H'(t)}{(1-\alpha t)H^2(t)}. \end{aligned} \tag{3.25}$$

Similarly differentiating T w.r.t 'y',

$$\begin{aligned} T &= \theta(\,\eta)\left(\frac{T_{\,0}}{1-\alpha t} + T_0\right), \\ \frac{\partial T}{\partial y} &= \frac{\partial}{\partial y}\left(\theta(\,\eta)\,\frac{T_{\,0}}{(1-\alpha t)} + T_0\right), \\ &= \frac{T_0\theta'(\eta)}{(1-\alpha t)}\frac{\partial \eta}{\partial y}, \\ \frac{\partial T}{\partial y} &= \frac{T_0\theta'(\eta)}{H(t)(1-\alpha t)}, \\ v\frac{\partial T}{\partial y} &= (v_H f(\eta))\left(\frac{T_0\theta'(\eta)}{H(t)(1-\alpha t)}\right), \\ v\frac{\partial T}{\partial y} &= \frac{v_H f(\eta) T_0\theta'(\eta)}{H(t)(1-\alpha t)}. \end{aligned} \tag{3.26}$$

(3.27)

Take (3.26) again differentiating w.r.t 'y',

$$\begin{aligned}\frac{\partial^2 T}{\partial y^2} &= \frac{\partial}{\partial y}\left(\frac{T_0\theta'(\eta)}{H(t)(1-\alpha t)}\right),\\ \frac{\partial^2 T}{\partial y^2} &= \frac{T_0\theta''(\eta)}{H^2(t)(1-\alpha t)},\\ \frac{k}{\rho c_p}\frac{\partial^2 T}{\partial y^2} &= \frac{k}{\rho c_p}\frac{T_0\theta''(\eta)}{H^2(t)(1-\alpha t)}.\end{aligned} \tag{3.28}$$

Using (3.25)-(3.28) in (3.24) becomes,

$$\frac{\theta(\eta)\alpha T_0}{(1-\alpha t)^2} - \frac{\theta'(\eta)T_0 y H'(t)}{(1-\alpha t)H^2(t)} + \frac{v_H f(\eta)T_0\theta'(\eta)}{H(t)(1-\alpha t)} = \frac{k}{\rho c_p}\frac{T_0\theta''(\eta)}{H^2(t)(1-\alpha t)}$$
$$+\frac{\nu}{c_p}\left(\frac{4v_H^2 f'^2(\eta)}{H^2}+\frac{x^2 v_H^2 f''^2(\eta)}{H^4}\right)+\frac{\sigma B_m^2}{\rho c_p}\left(\frac{-xv_H f'(\eta)}{H}\sin\gamma - v_H f(\eta)\cos\gamma\right)^2.$$

Multiplying $\frac{H^2(t)(1-\alpha t)\rho c_p}{kT_0}$ on both sides, the dimensionless form of (3.24) can be reduced:

$$\theta'' + SPr(f\theta' - \eta\theta' - 2\theta) + PrEc\Big[f''^2 + 4\delta^2 f'^2 + M^2(f'^2 sin^2\gamma +$$
$$\delta^2 f^2\cos^2\gamma + 2\delta f f'\sin\gamma\cos\gamma)\Big]. \tag{3.29}$$

Now for converting the associated boundary conditions into the dimensionless form, the following steps have been taken:

- $u = u_s \quad at \quad y = 0.$
  $$\frac{-xv_H f'(\eta)}{H(t)} = u_s \quad at \quad \eta = 0.$$
  $$f'(\eta) = \frac{u_s H(t)}{-xv_H},$$
  $$f'(0) = \frac{u_s\delta}{v_H},$$
  $$f'(0) = R.$$
- $v = \dfrac{-v_0}{\sqrt{1-\alpha t}} \quad at \quad y = 0.$
  $$v_H f(\ \eta\ ) = \frac{-v_0}{\sqrt{1-\alpha t}} \quad at \quad \eta = 0.$$
  $$f(0) = \frac{-v_0}{v_H\sqrt{1-\alpha\ t}},$$

$$f(0) = \frac{2v_0}{\alpha l},$$
$$f(0) = s_b.$$

- $T = T_0 \quad at \quad y = 0.$
  $$\theta(\eta)\left(\frac{T_0}{1-\alpha t}\right) + T_0 = T_0 \quad at \quad \eta = 0.$$
  $$\theta(0)\left(\frac{T_0}{1 - \alpha\, t}\right) = 0,$$
  $$\theta(0) = 0.$$

- $u = 0 \quad at \quad y = H(t).$
  $$\frac{-xv_H f'(\eta)}{H(\,t\,)} = 0 \quad at \quad \eta = 1.$$
  $$f'(1) = 0.$$
- $v = v_H \quad at \quad y = H(t).$
  $$v_H f(\eta) = v_H \quad at \quad \eta = 1.$$
  $$f(1) = 1.$$
- $T = T_0 + \frac{T_0}{1 - \alpha\, t} \quad at \quad y = H(t).$
  $$\theta(\eta)\left(\frac{T_0}{1-\alpha t}\right) + T_0 = T_0 + \frac{T_0}{1-\alpha t} \quad at \quad \eta = 1.$$
  $$\theta\,(1)\left(\frac{T_0}{1 - \alpha\, t}\right) = \frac{T_0}{1-\alpha t},$$
  $$\theta\,(1) = 1.$$

The final dimensionless form of the governing model is

$$f^{(iv)} - S\,(\eta f''' + 3f'' + f'f' - ff''') - M^2\,\sin\gamma\,(\sin\gamma\, f'' + 2\delta\,\cos\gamma\, f') = 0. \quad (3.30)$$

$$\theta'' + SPr(\, f\,\theta' - \eta\theta' - 2\theta) +$$
$$PrEc\Big[f''^2 + 4\delta^2 f'^2 + M^2\,(f'^{\,2}\,\sin^2\gamma + \delta^2\, f^{\,2}\,\cos^2\,\gamma + 2\delta f\, f'\,\sin\gamma\cos\gamma)\Big] = 0. \quad (3.31)$$

The associated boundary conditions of (3.5) and (3.6) shown as:

$$f'(\eta) = R\,, \quad f(\eta) = S_b\,, \quad \theta(\eta) = 0, \quad \text{at} \quad \eta = 0, \tag{3.32}$$

$$f'(\eta) = 0\,, \quad f(\eta) = 1\,, \quad \theta(\eta) = 1, \quad \text{at} \quad \eta = 1. \tag{3.33}$$

Different parameters used in (3.30) and (3.31) are defined as:

$$\left.\begin{aligned} S = \frac{\alpha l^2}{2\nu}, \quad Pr = \frac{\mu C_p}{k}, \quad Ec = \frac{u_0^2}{C_p R^2 (T_H - T_0)}, \\ M^2 = \frac{\sigma B_0^2 l^2}{\rho\nu}, \quad S_b = \frac{2v_0}{\alpha l}, \quad R = \frac{u_s \delta}{v_H}, \delta = \frac{H}{x}. \end{aligned}\right\} \tag{3.34}$$

3.2 Physical Quantities

The skin friction (C_f) and the Nusselt number (Nu) are the main physical quantities, we discussed here.

The skin friction C_f are expressed as:

$$\begin{aligned} C_f &= \frac{\mu(\frac{\partial u}{\partial y})_{y=H(t)}}{\rho v_H^2} \\ C_f &= \frac{\nu(\frac{\partial u}{\partial y})_{y=H(t)}}{v_H^2} \\ u &= \frac{\alpha x f'(\eta)}{2(1-\alpha t)} \\ \frac{\partial u}{\partial y} &= \frac{\alpha x f''(\eta)}{2(1-\alpha t)} \left(\frac{\partial \eta}{\partial y}\right) \\ &= \frac{\alpha x f''(\eta)}{2(1-\alpha t)} \left(\frac{1}{l(1-\alpha t)^{1/2}}\right) \\ \frac{\partial u}{\partial y} &= \frac{\alpha x f''(\eta)}{2l(1-\alpha t)^{3/2}} \\ C_f &= \frac{\nu\left(\frac{\alpha x f''(\eta)}{2l(1-\alpha t)^{3/2}}\right)}{\left(\frac{-\alpha l}{2\sqrt{1-\alpha t}}\right)^2} \\ &= \nu\left(\frac{\alpha x f''(\eta)}{2l(1-\alpha t)^{3/2}}\right)\left(\frac{4(1-\alpha t)}{\alpha^2 l^2}\right) \\ C_f &= \frac{2x\nu f''(\eta)}{\alpha l^3 (1-\alpha t)^{1/2}} \end{aligned} \tag{3.35}$$

$$
\begin{aligned}
C_f &= \frac{2x\nu f''(\eta)}{\alpha l^3(1-\alpha t)^{1/2}}\left(\frac{bx(1-\alpha t)}{bx(1-\alpha t)}\right) \quad \left(\because u_s = \frac{bx}{1-\alpha t}\right) \\
&= \frac{2bx^2\nu f''(\eta)}{\alpha l^3(1-\alpha t)^{3/2}}\left(\frac{(1-\alpha t)}{bx}\right) \\
&= \frac{2bx^2\nu f''(\eta)}{\alpha l^3(1-\alpha t)^{3/2}}\left(\frac{1}{u_s}\right) \\
&= \frac{2bx^3 f''(\eta)}{\alpha l^3(1-\alpha t)^{3/2}}\left(\frac{\nu}{u_s x}\right) \\
&= \frac{2bx^3 f''(\eta)}{\alpha l^3(1-\alpha t)^{3/2}}\left(\frac{1}{Re_x}\right) \\
f''(\eta) &= \frac{\alpha l^3(1-\alpha t)^{3/2}}{2bx^3} Re_x C_f \quad \text{at} \quad \eta = 1,
\end{aligned} \tag{3.36}
$$

where $Re_x = \frac{u_s x}{\nu}$ represents the local Reynolds number.

The Nusselt number Nu at the lower plate surface may be expressed as:

$$
Nu = \frac{l}{T_H - T_0}\left(\frac{\partial T}{\partial y}\right)_{y=H(t)} \tag{3.37}
$$

Consider T and differetiate w.r.t y,

$$
\begin{aligned}
T &= \left(\frac{T_0\theta(\eta)}{1-\alpha t}\right) + T_0 \\
\frac{\partial T}{\partial y} &= \left(\frac{T_0}{1-\alpha t}\right)\theta'(\eta)\frac{1}{l(1-\alpha t)^{1/2}} \\
\frac{\partial T}{\partial y} &= \frac{T_0\theta'(\eta)}{l(1-\alpha t)^{3/2}} \\
Nu &= \frac{l}{T_H - T_0}\left(\frac{T_0\theta'(\eta)}{l(1-\alpha t)^{3/2}}\right) \\
Nu &= \frac{1}{T_H - T_0}\left(\frac{T_0\theta'(\eta)}{(1-\alpha t)^{3/2}}\right) \quad \because \left(T_H - T_0 = \frac{T_0}{1-\alpha t}\right) \\
Nu &= \frac{(1-\alpha t)}{T_0}\left(\frac{T_0\theta'(\eta)}{(1-\alpha t)^{3/2}}\right) \\
Nu &= \frac{\theta'(\eta)}{(1-\alpha t)^{1/2}} \\
\theta'(\eta) &= Nu\left((1-\alpha t)^{1/2}\right) \\
\theta'(\eta) &= Nu\left(\frac{(1-\alpha t)^{1/2}}{(bx)^{1/2}}(bx)^{1/2}\right)
\end{aligned}
$$

$$\theta'(\eta) = Nu\left(\frac{(bx)^{1/2}}{(u_s)^{1/2}}\right) \qquad \because \left(u_s = \frac{bx}{1-\alpha t}\right)$$
$$\theta'(\eta) = Nu\left(\frac{b^{1/2}x}{(u_s x)^{1/2}}\right)$$
$$\theta'(\eta) = Nub^{1/2}x\frac{\nu^{1/2}}{(u_s x)^{1/2}}\frac{1}{\nu^{1/2}}$$
$$\theta'(\eta) = \frac{Nub^{1/2}x}{\nu^{1/2}}\frac{1}{(Re_x)^{1/2}}$$
$$\theta'(\eta) = \left(\frac{\nu}{b}\right)^{-1/2} x(Re_x)^{-1/2}Nu \quad at \quad \eta = 1, \tag{3.38}$$

where Re_x denotes the local Reynolds number and is define as $Re_x = \frac{u_s x}{\nu}$.

3.3 Solution Methodology

For the solution of ODEs, (3.30) and (3.31), the shooting method has been used. The missing ICs $f''(0)$, $f'''(0)$ and $\theta'(0)$ are denoted by χ_1, χ_2 and χ. For further refining of the missing conditions, Newton's method will be used. Furthermore, the following notations have been used.

$$\Rightarrow \quad f = f_1\,, \quad f' = f_2\,, \quad f'' = f_3\,, \quad f''' = f_4\,, \quad f^{(iv)} = f_4'$$
$$\frac{\partial f_1}{\partial \chi_1} = f_5, \quad \frac{\partial f_2}{\partial \chi_1} = f_6, \quad \frac{\partial f_3}{\partial \chi_1} = f_7, \quad \frac{\partial f_4}{\partial \chi_1} = f_8$$
$$\frac{\partial f_1}{\partial \chi_2} = f_9, \quad \frac{\partial f_2}{\partial \chi_2} = f_{10}, \quad \frac{\partial f_3}{\partial \chi_2} = f_{11}, \quad \frac{\partial f_4}{\partial \chi_2} = f_{12}$$
$$\Rightarrow \quad \theta = Y_1, \quad \theta' = Y_2, \quad \theta'' = Y_2'$$
$$\frac{\partial Y_1}{\partial \chi} = Y_3, \quad \frac{\partial Y_2}{\partial \chi} = Y_4$$

The above mathematical problem model (3.30) and (3.31), can now be given as first order ODEs in the following form.

$$f_1' = f_2 \qquad f_1(0) = 0.1,$$
$$f_2' = f_3 \qquad f_2(0) = 0.5,$$
$$f_3' = f_4 \qquad f_3(0) = \chi_1,$$

$$
\begin{aligned}
f_4' &= S(\eta f_4 + 3f_3 + f_2 f_3 - f_1 f_4) + M^2 \sin\gamma(\sin\gamma f_3 + 2\delta\cos\gamma f_2) && f_4(0) = \chi_2,\\
f_5' &= f_6 && f_5(0) = 0,\\
f_6' &= f_7 && f_6(0) = 0,\\
f_7' &= f_8 && f_7(0) = 1,\\
f_8' &= S(\eta f_8 + 3f_7 + f_2 f_7 + f_3 f_6 - f_1 f_8 - f_4 f_5)\\
&\quad + M^2 \sin\gamma(f_7 \sin\gamma + 2\delta f_6 \cos\gamma) && f_8(0) = 0,\\
f_9' &= f_{10} && f_9(0) = 0,\\
f_{10}' &= f_{11} && f_{10}(0) = 0,\\
f_{11}' &= f_{12} && f_{11}(0) = 0,\\
f_{12}' &= S(\eta f_{12} + 3f_{11} + f_2 f_{11} + f_{10} f_3 - f_1 f_{12} - f_4 f_9)\\
&\quad + M^2 \sin\gamma(f_{11} \sin\gamma + 2\delta f_{10} \cos\gamma) && f_{12}(0) = 1,\\
Y_1' &= Y_2 && Y_1\ (0) = 0,\\
Y_2' &= -PrS(fY_2 - \eta Y_2 - 2Y_1) - PrEc[f''^2 + 4\delta^2 f'^2\\
&\quad + M^2\ (f'^2\ \sin^2\gamma\ +\ f^2\delta^2\cos^2\gamma + 2ff'\delta\ \sin\gamma\ \cos\gamma)] && Y_2\ (0) = \chi,\\
Y_3' &= Y_4 && Y_3\ (0) = 0,\\
Y_4' &= -PrS(fY_4 - \eta Y_4 - 2Y_3) && Y_4\ (0) = 1,
\end{aligned}
$$

The above IVP is numerically solved by RK4 method. To obtain the approximate solution, the problem domain was taken as [0 , 1]. In the above system of equations, the missing conditions χ_1, χ_2, and χ are to be chosen such that

$$f_1(1\ ,\ \chi_1\ ,\ \chi_2)\ =\ 0, \quad f_2(1\ ,\ \chi_1\ ,\ \chi_2) = 0, \quad Y_1(1\ ,\ \chi) = 0. \tag{3.39}$$

Newton's approach was applied to carry out the following iterative scheme for the refinement of the missing conditions:

$$\begin{bmatrix} {\chi_1}^{(n\ +\ 1)} \\ {\chi_2}^{(n\ +\ 1)} \end{bmatrix} = \begin{bmatrix} {\chi_1}^{(\ n\ )} \\ {\chi_2}^{(\ n\ )} \end{bmatrix} - \begin{bmatrix} f_5 & f_9 \\ f_6 & f_{10} \end{bmatrix}^{-1} \begin{bmatrix} {f_1}^{(\ n\ )} \\ {f_2}^{(\ n\ )} \end{bmatrix}_{(\chi_1^{(n)}, \chi_2^{(n)}, 1)}$$

and

$$\chi_{n+1} = \chi_n - \frac{Y_1(1,\chi) - 1}{Y_3(1,\chi)}, \tag{3.40}$$

1. Choice of the guesses $\chi_1 = \chi_1^{(0)}$, $\chi_2 = \chi_2^{(0)}$, and $\chi = \chi^{(0)}$.

2. Choosing a small positive number ϵ.
   If $max\{|f_1(1,\ \chi_1,\ \chi_2) - 1|, |f_2(1,\ \chi_1,\ \chi_2)\ -\ 0|\} < \epsilon$, stop the process otherwise go to (3).

3. Calculating ${\chi_1}^{(n\ +\ 1)}$ and ${\chi_2}^{(n\ +\ 1)}$, $\quad n = 0, 1, 2, 3...$ by using Newton scheme.
   If $max|Y_1(1\ ,\ \chi) - 1| < \epsilon$, stop the process otherwise go to (4).

4. Compute $\chi^{(n\ +\ 1)}$, $n = 0, 1, 2, 3...$ by using Newton scheme.
   where $\epsilon = 10^{-10}$ is the tolerance for the modeled problem.

3.4 Graphical Results

In order to show the squeezing movement more accurately, the computed results are presented and discussed graphically. Figures 3.2-3.12 shows the variations in velocity and temperature curves against some of the parameters including squeeze parameter S, the inclination angle γ, the magnetic parameter M, the lower plate stretching parameter R, the Eckert number Ec and the parameter for lower plate suction/injection.

Figure 3.2 and 3.3 indicate the squeeze number effect on velocity and temperature. Figure 3.2 demonstrates the distribution of fluid velocity close to the lower or upper end of plates are decreasing due to rising of the squeeze number, but for the velocity an opposite effect has been observed close to the centre between the plates. It is noted from Figure 3.3 that rising the values of the squeezing parameter causes reduction in the temperature. When the plates move close to each other, the temperature field will be comparatively high.

Figure 3.4 and 3.5 represent the velocity and temperature of the fluid for various magnetic parameter values. It has been observed in Figure 3.4 that an increase in the magnetic parameter causes the fluid velocity to increase at both ends (lower and upper) of the plates, but the fluid velocity near the center, quite slightly, shows a noticeable decrease. The fluid in the central regions has larger Lorentz force than the fluid near the plate. The reason is that the Lorentz force in fluid motion presents resistance. So excessive Lorentz forces make velocity slow down close the central region of plates. Figure 3.5 shows that the fluid temperature rises from the lower to upper plate surface when the magnetic field parameter rises. For the larger magnetic value, the fluid temperature increases not only near the upper surface but also in the centre between the plates. Actually, the strong magnetic field affects the temperature distribution in the regions. Large friction along with a strong magnetic field generates more heat in fluids.

Velocity and temperature profiles variations were shown through Figure 3.6 and 3.7 by rising value of the magnetic angle. The angle of magnetic inclination ranges between 0 and $\pi/2$. Similar profiles behaviors of velocity and temperature were obtained from both figures when compared to the corresponding profiles of different magnetic parameter values. The angle of magnetic field inclination γ effects on both the fluid velocity and the temperature are similar to those of the magnetic parameter. Therefore, the transfer of fluid in the squeezing movement in practical applications related to momentum and heat control, the affects generated by changing the strength of the magnetic field can also be obtained by modifying the angle of magnetic field inclination.

Figure 3.8 and 3.9 show the affect of stretching parameter of the lower-plate on the velocity and temperature. In Figure 3.8 the fluid velocity increases close to the lower plate as compared to the fluid velocity close to the upper plate. Furthermore, as the stretching parameter on the lower surface rises slowly, the maximum value of velocity can be seen in the surface of lower plate. Figure 3.9 reflects that when we rise the stretching parameter of the lower plate, the fluid temperature above

the lower plate decreases and increases thereafter, when we take the stretching parameter $R > 1.5$ the fluid temperature close to the upper plate at first increases and then steadily decreases.

Figure 3.10 and 3.11 represent the effects of lower-plate suction/injection parameter on the fluid velocity and temperature profiles. Figure 3.10 indicates a decline in velocity for the lower plate suction/injection parameter. In fact, as the lower plate stretches for greater suction across the lower plate, the maximum fluid velocity does not show between the centre of the plates, and subsequently fluid velocity reduces from the lower to upper surface of the plate. In order to increase the suction/injection parameter, the temperature profiles decrease. In particular, it was noted that as the suction/injection parameter S_b reduces, the maximum fluid temperature does not occur on the upper surface of the plate but in the centre region between the two plates.

The temperature for different values of Eckert number was shown in Figure 3.12. A clear temperature rise is observed to increase the values of Eckert number. This increase in the thermal field is evident because Eckert has directly affects on the process of heat dissipation, which in turn increases the temperature field between the plates. Figure 3.12 also indicates that the maximum fluid temperature occurs in the centre between the two plates for larger Eckert number, whereas it tends to be smaller in the upper plate.

Figure 3.13 and 3.14 demonstrate the effects of the squeeze parameter and magnetic angle on the coefficient of skin friction and the Nusselt number, where the magnetic inclination angle ranges among 0^0 to 90^0. The absolute value of skin friction and Nusselt number may be noticed as a decreasing function of the angle of magnetic inclination γ. In addition, for the increment of squeeze parameter and the angle of magnetic inclination are fixed, then the Nusselt number increases and skin friction coefficient decreases.

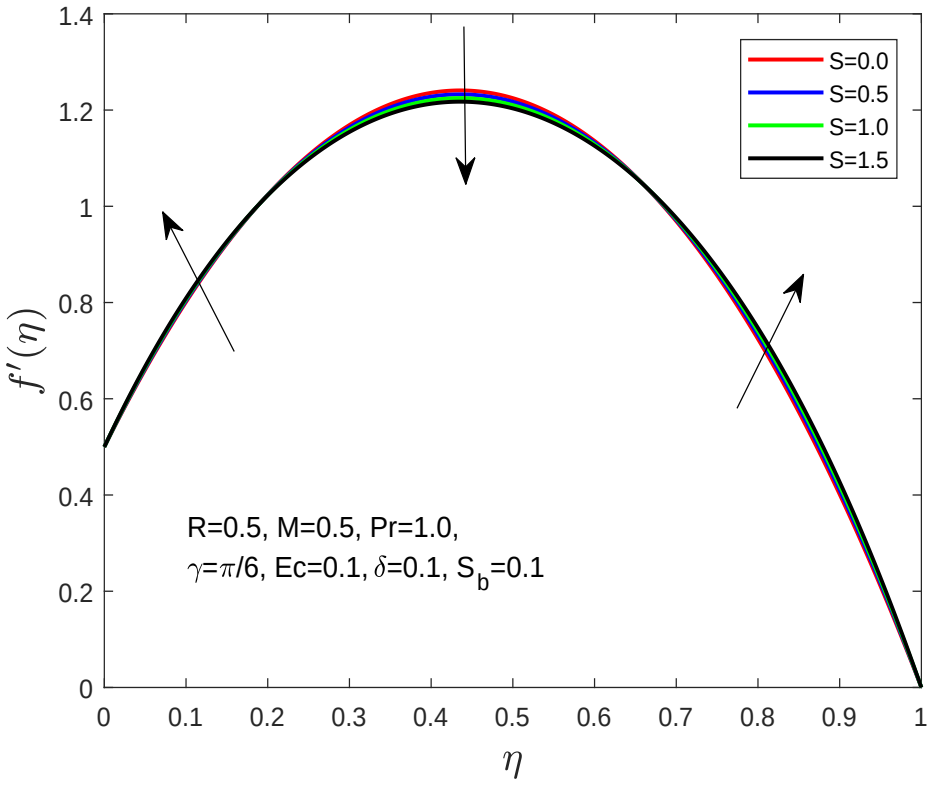

Figure 3.2: Effect of S on the f'.

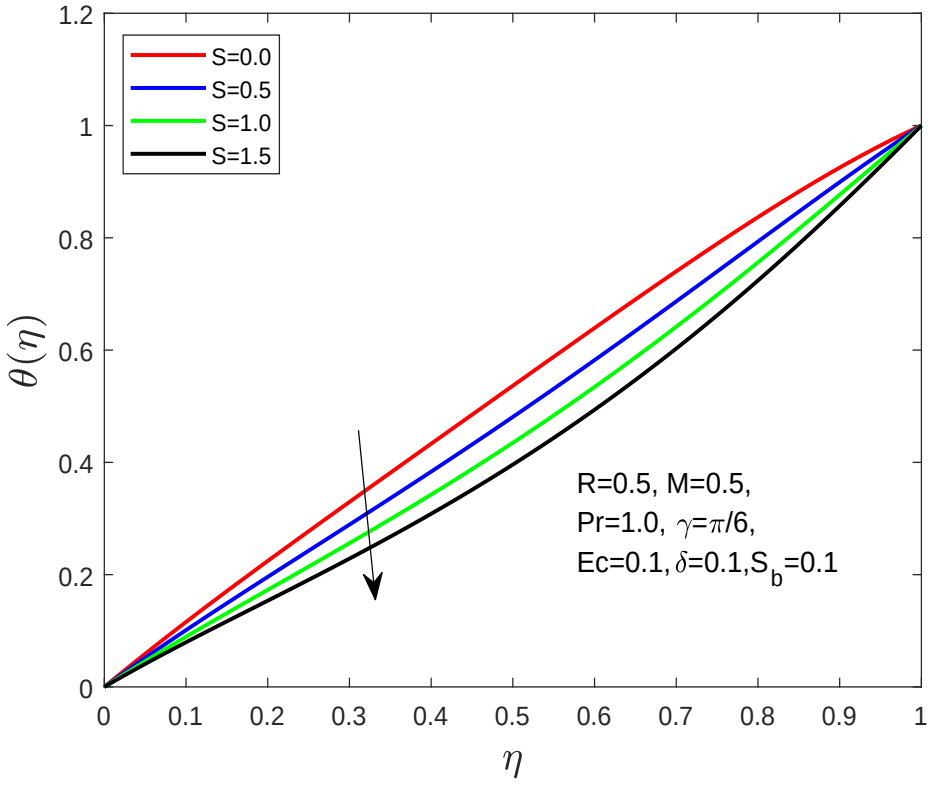

Figure 3.3: Effect of S on the $\theta(\eta)$.

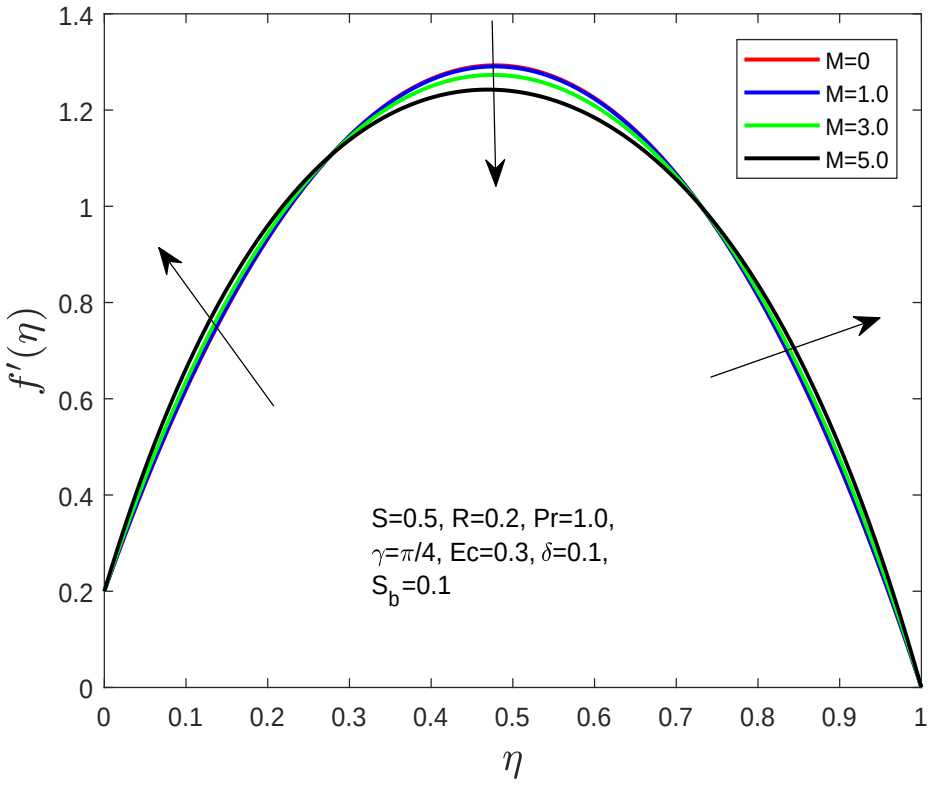

Figure 3.4: Effect of M on the f'.

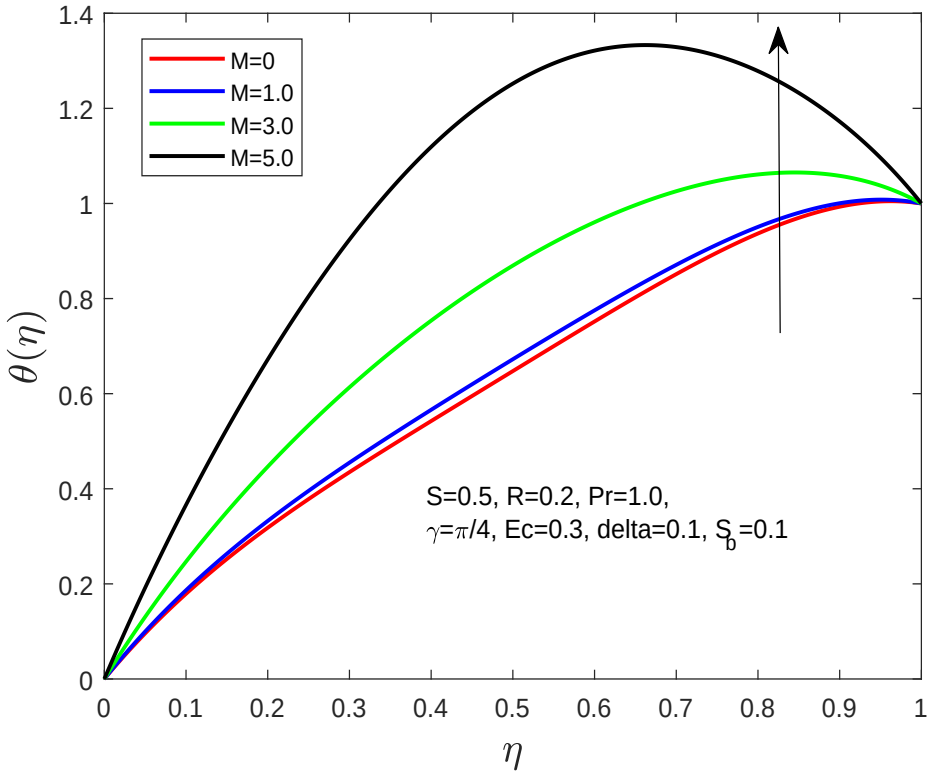

Figure 3.5: Effect of M on the $\theta(\eta)$.

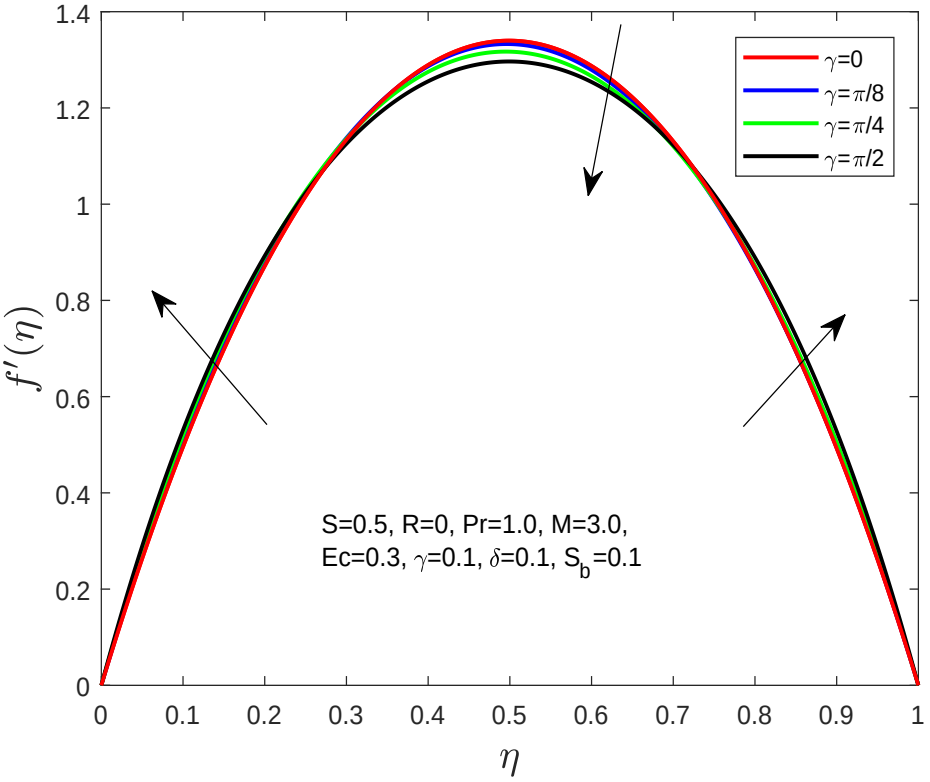

Figure 3.6: Effect of γ on the f'.

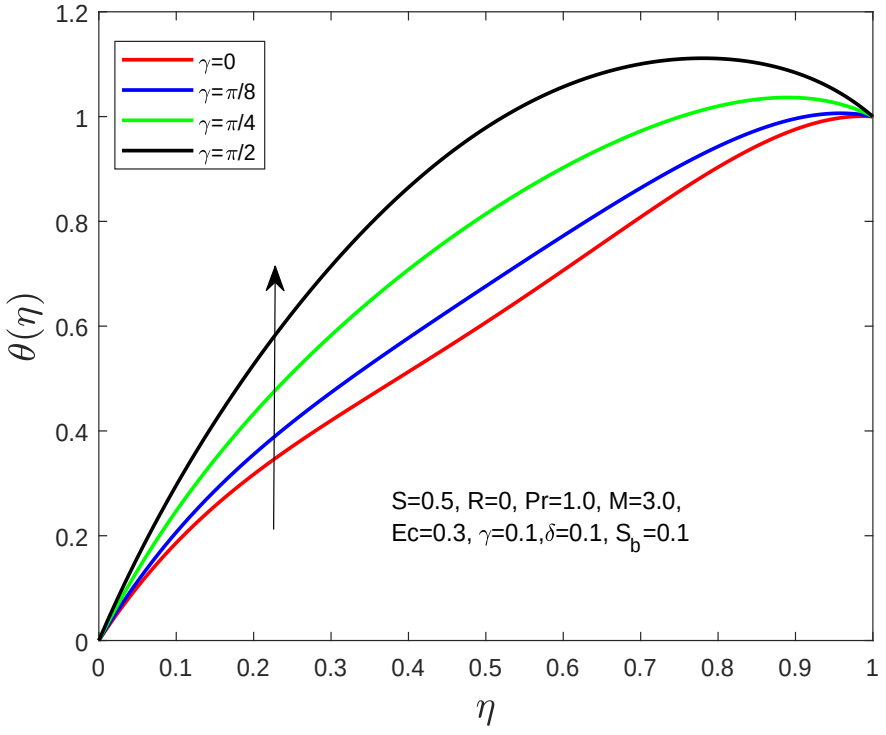

Figure 3.7: Effect of γ on the $\theta(\eta)$.

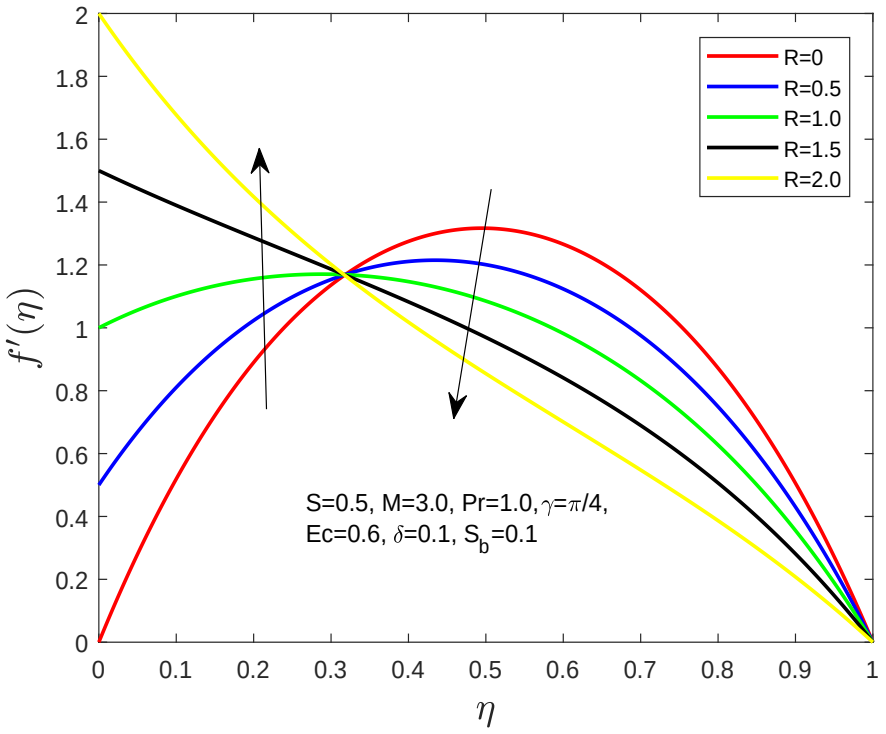

Figure 3.8: Effect of R on the f'.

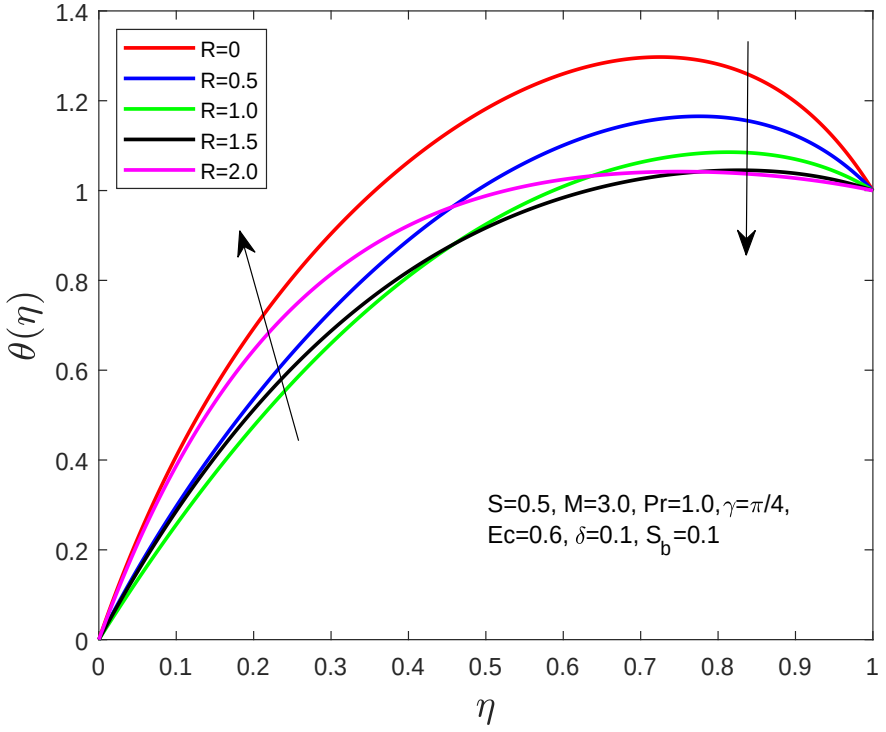

Figure 3.9: Effect of R on the $\theta(\eta)$.

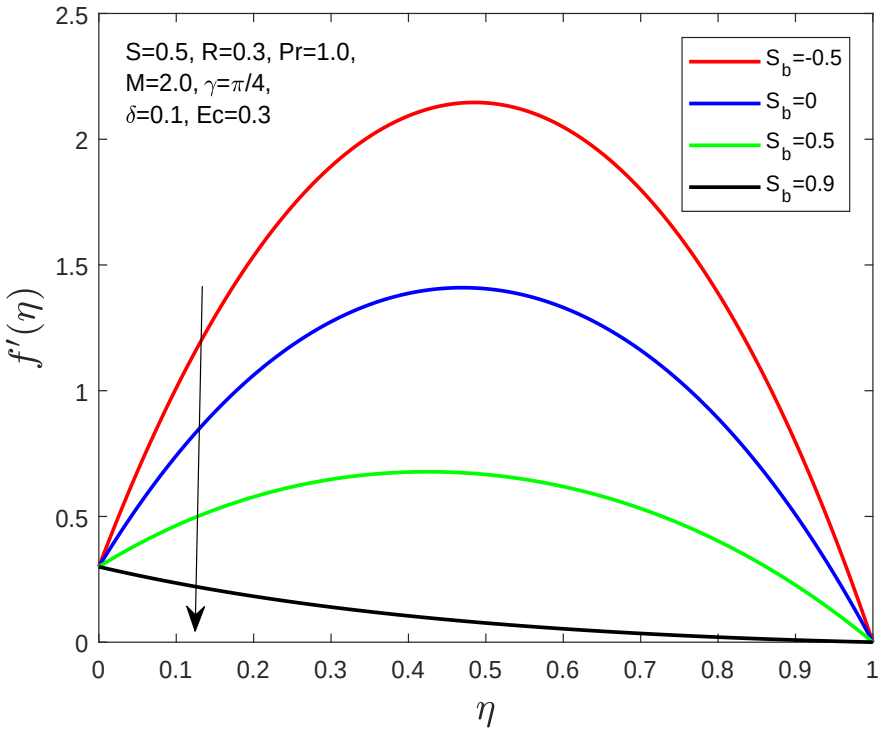

Figure 3.10: Effect of S_b on the f'.

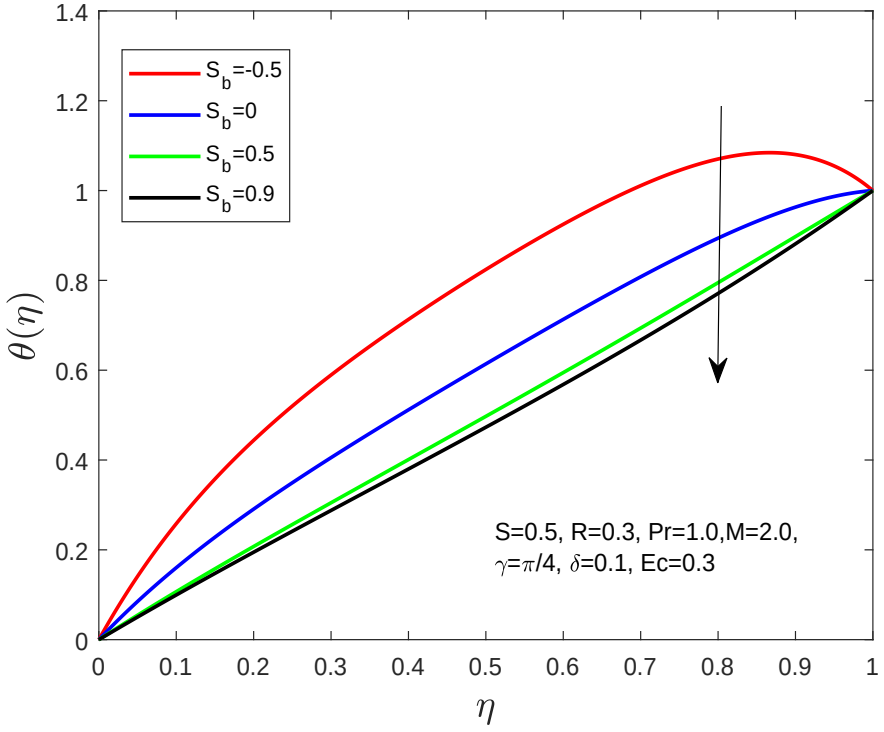

Figure 3.11: Effect of S_b on the $\theta(\eta)$.

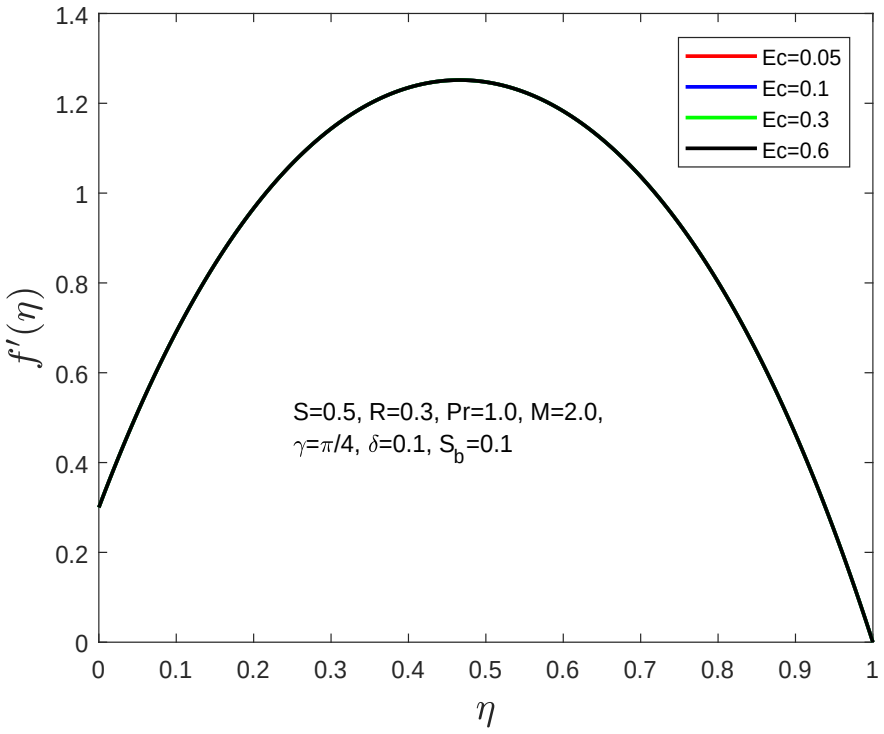

Figure 3.12: Effect of Ec on the f'.

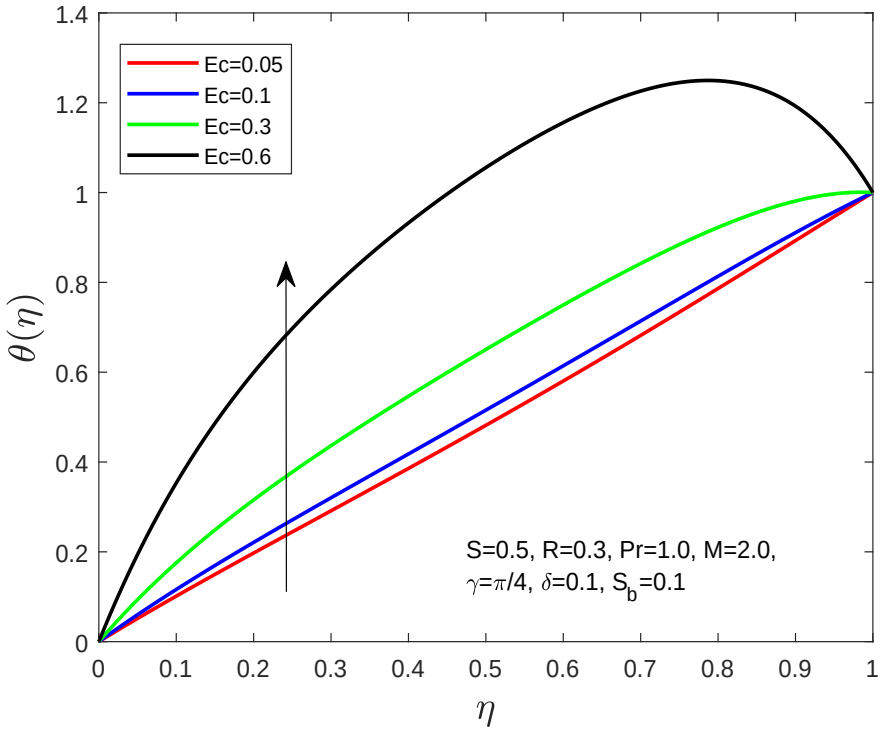

Figure 3.13: Effect of Ec on the $\theta(\eta)$.

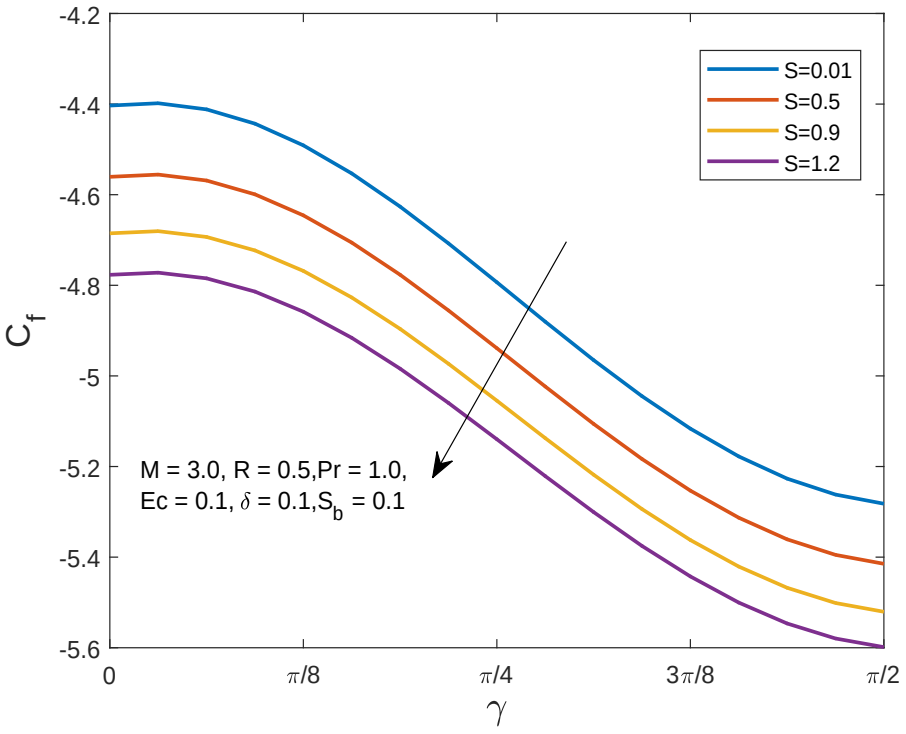

Figure 3.14: Effect of S and γ on the C_f.

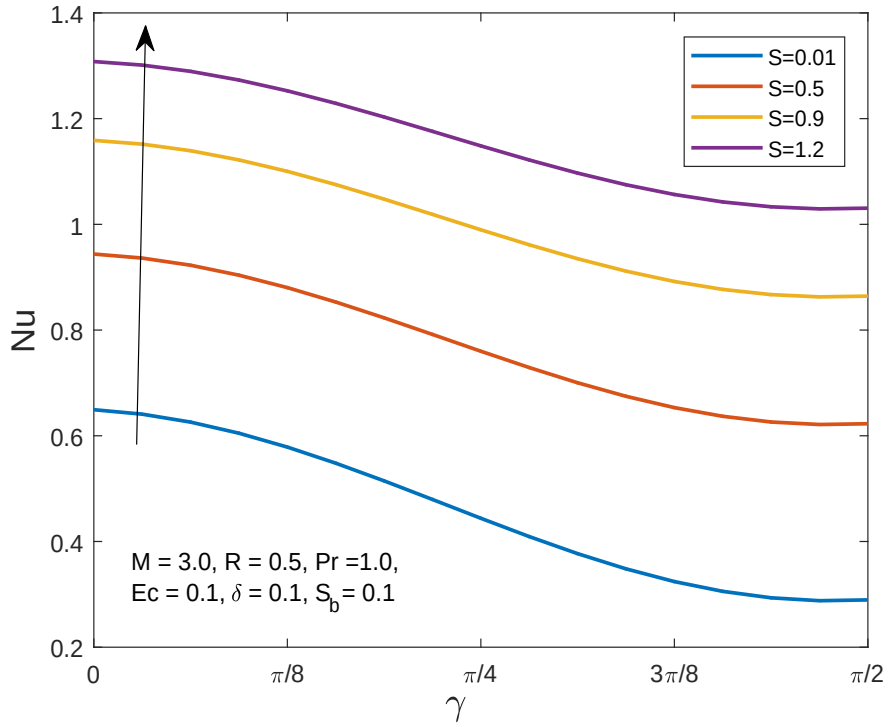

Figure 3.15: Effect of S and γ on Nu.

3.5 Summary

The analysis showed the affects of a magnetic field on unsteady two-dimensional squeezing movement of viscous fluid bounded between two infinite parallel plates. Main points have been presented below:

- Squeeze parameter and temperature of the fluid are inversely proportional to each other. The increment in the squeeze parameter allows fluid temperature to decrease.
- Increase in temperature with increasing magnetic parameter, inclination angle of magnetic field or the Eckert number.
- The fluid having the maximum temperature can be seen in the centre between the plates for smaller squeezing parameter or larger magnetic parameter.
- The effects on the velocities and temperature generated by changing the strength of the magnetic field can also be obtained by modifying the magnetic field inclination angle γ.
- Increasing the stretching parameter results in an increase in velocity and fluid temperature near the lower plate where there is an opposite pattern seen near the upper plate.

Chapter 4

Effects of a Magnetic Field on Unsteady Squeezing Flow in a Porous Medium

This chapter contains the extension of [46], modeling and investigating an unsteady squeezing movement of viscous fluid between two infinite parallel plates that passes in a porous medium with the effect of radiative heat flux model. Problematic applications are used in hydraulic machinery and equipment, electric motors, food processing, and engines for automobiles. The governing system of nonlinear PDEs is converted into a model of nonlinear ODEs by utilizing the transformation of similarities. Numerical results are obtained for the set of nonlinear ODEs by utilizing shooting technique together with Runge-Kutta method of order four (RK4). Finally, the results are presented through the graphs for different parameters.

4.1 Mathematical Modeling

We considered the problem of an unsteady two-dimensional squeezing movement between infinite parallel plates that are subject to an inclined magnetic field **B** as shown in Figure 3.1. The both plates are located at $H(t) = l\sqrt{1 - \alpha t}$. When

$\alpha < 0$ as the plates move apart and for $\alpha > 0$, the two plates are squeezed. There is also consideration of the effect of nonlinear thermal radiation.

The governing PDEs are given by:

$$\frac{\partial u}{\partial x} + \frac{\partial v}{\partial y} = 0, \tag{4.1}$$

$$\frac{\partial u}{\partial t} + u\,\frac{\partial u}{\partial x} + v\,\frac{\partial u}{\partial y} = -\frac{1}{\rho}\frac{\partial p}{\partial x} + \frac{\mu}{\rho}\left(\frac{\partial^2 u}{\partial x^2} + \frac{\partial^2 u}{\partial y^2}\right) + \frac{\sigma B_m^2}{\rho}\sin\gamma(v\,\cos\gamma - u\,\sin\gamma) - \frac{\mu}{\rho}\left(\frac{u}{k^*}\right), \tag{4.2}$$

$$\frac{\partial v}{\partial t} + u\,\frac{\partial v}{\partial x} + v\,\frac{\partial v}{\partial y} = -\frac{1}{\rho}\frac{\partial p}{\partial y} + \frac{\mu}{\rho}\left(\frac{\partial^2 v}{\partial x^2} + \frac{\partial^2 v}{\partial y^2}\right) + \frac{\sigma B_m^2}{\rho}\cos\gamma(\,u\,\sin\gamma - v\,\cos\gamma) - \frac{\mu}{\rho}\left(\frac{v}{k^*}\right), \tag{4.3}$$

$$\begin{aligned}\frac{\partial T}{\partial t} + u\,\frac{\partial T}{\partial x} + v\,\frac{\partial T}{\partial y} &= \frac{k}{\rho c_p}\left(\frac{\partial^2 T}{\partial x^2} + \frac{\partial^2 T}{\partial y^2}\right) \\ &+ \frac{\mu}{\rho c_p}\left[2\left(\frac{\partial u}{\partial x}\right)^2 + 2\left(\frac{\partial v}{\partial y}\right)^2 + \left(\frac{\partial u}{\partial y} + \frac{\partial v}{\partial x}\right)^2\right] \\ &+ \frac{\sigma B_m^2}{\rho c_p}(u\sin\gamma - v\cos\gamma)^2 - \frac{1}{\rho c_p}\frac{\partial q_r}{\partial y}.\end{aligned} \tag{4.4}$$

4.1.1 Dimensional Boundary Conditions

The dimensional form of the BCs is:

$$u = u_s = \frac{bx}{1-\alpha t}, \quad v = v_c = -\frac{v_0}{\sqrt{1-\alpha t}}, \quad T = T_0 \quad \text{at} \quad y = 0, \tag{4.5}$$

$$u = 0, v = v_H = \frac{dH}{dt} = -\frac{\alpha l}{2\sqrt{1-\alpha t}}, \quad T = T_H = T_0 + \frac{T_0}{1-\alpha t} \text{ at } y = H(t). \tag{4.6}$$

The flux of radiative heat is given by:

$$q_r = -\frac{4}{3}\frac{\sigma^*}{k^*}\frac{\partial T^{\,4}}{\partial y}, \tag{4.7}$$

where σ^* is the Stefan-Boltzmann constant and k^* is the coefficient of mean absorption. By applying Taylor series for temperature of free stream and ignoring higher-order values, we get

$$T^{\,4} \;=\; 4T\;T_H^3 - 3T_H^4. \tag{4.8}$$

Substituting (4.8) in (4.7), becomes

$$q_r = -\frac{16\sigma^* T_H^3}{3k^*}\frac{\partial T}{\partial y}, \tag{4.9}$$

Substituting (4.9) in (4.4), we get final form of energy equation is:

$$\begin{aligned}\frac{\partial T}{\partial t} \;+\; u\,\frac{\partial T}{\partial x} \;+\; v\,\frac{\partial T}{\partial y} \;&=\; \frac{k}{\rho c_p}\left(\frac{\partial^2 T}{\partial x^2} \;+\; \frac{\partial^2 T}{\partial y^2}\right)\\ &+ \frac{\mu}{\rho c_p}\left[2\,\left(\frac{\partial u}{\partial x}\right)^{2} + 2\,\left(\frac{\partial v}{\partial y}\right)^{2} + \left(\frac{\partial u}{\partial y} + \frac{\partial v}{\partial x}\right)^{2}\right]\\ &+ \frac{\sigma B_m^2}{\rho c_p}(u\sin\gamma - v\cos\gamma)^2 + \frac{16\sigma^* T_H^3}{3k^*\rho c_p}\frac{\partial^2 T}{\partial y^2}.\end{aligned} \tag{4.10}$$

For the conversion of the modeled equations (4.1), (4.2), (4.3) and (4.10) into the dimensionless form, the given below is the similarity transformation that defined in [46] has been used:

$$\eta = \frac{y}{l(1-\alpha t)^{1/2}}, \quad v = v_H f(\eta), \quad u = -\frac{x v_H f'(\eta)}{l(1-\alpha t)^{1/2}}, \quad \theta(\eta) = \frac{T - T_0}{T_H - T_0}. \tag{4.11}$$

The detailed procedure for the conversion of continuity equation (4.1) has been discussed in Chapter 3.

Now we include the procedure for the conversion of (4.2) and (4.3) into dimensionless form.

Converting PDEs of momentum equations into ODE to utilize transformation of similarities, so differentiating (4.2) w.r.t 'y' and (4.3) w.r.t 'x' and subtracting both eqs to eliminate the pressure gradient we proceed as follows.

$$\frac{\partial}{\partial y}\left(\frac{\partial u}{\partial t}+u\frac{\partial u}{\partial x}+v\frac{\partial u}{\partial y}\right)-\frac{\partial}{\partial x}\left(\frac{\partial v}{\partial t}+u\frac{\partial v}{\partial x}+v\frac{\partial v}{\partial y}\right)=-\frac{1}{\rho}\frac{\partial^2 p}{\partial y\,\partial x}$$
$$+\frac{1}{\rho}\frac{\partial^2 p}{\partial x\,\partial y}+\nu\frac{\partial}{\partial y}\left(\frac{\partial^2 u}{\partial x^2}+\frac{\partial^2 u}{\partial y^2}\right)-\nu\frac{\partial}{\partial x}\left(\frac{\partial^2 v}{\partial x^2}+\frac{\partial^2 v}{\partial y^2}\right)$$
$$+\frac{\sigma B_m^2}{\rho}\left[\sin\gamma\frac{\partial}{\partial y}(v\cos\gamma-u\sin\gamma)-\cos\gamma\frac{\partial}{\partial x}(u\sin\gamma-v\cos\gamma)\right]$$
$$-\frac{\nu}{k^*}\frac{\partial u}{\partial y}+\frac{\nu}{k^*}\frac{\partial v}{\partial x}. \tag{4.12}$$

'v' does not depend on x so the derivative of v is zero and second derivative of u is also zero.

$$v=v_H f(\eta)\quad;\quad u=-\frac{x v_H f'(\eta)}{H(t)},$$

$$\frac{\partial v}{\partial x}=0\quad;\quad\frac{\partial^2 u}{\partial x^2}=0.$$

So we have,

$$\frac{\partial}{\partial y}\left(\frac{\partial u}{\partial t}+u\frac{\partial u}{\partial x}+v\frac{\partial u}{\partial y}\right)=\nu\frac{\partial^3 u}{\partial y^3}+\frac{\sigma B_m^2}{\rho}\sin\gamma\ \cos\gamma\ \frac{\partial v}{\partial y}-\frac{\sigma B_m^2}{\rho}\sin^2\gamma\frac{\partial u}{\partial y}$$
$$-\frac{\sigma B_m^2}{\rho}\sin\gamma\ \cos\gamma\ \frac{\partial u}{\partial x}-\frac{\nu}{k^*}\frac{\partial u}{\partial y},$$

$$\frac{\partial^2 u}{\partial y\partial t}+u\frac{\partial^2 u}{\partial y\partial x}+v\frac{\partial^2 u}{\partial y^2}=\nu\frac{\partial^3 u}{\partial y^3}+\frac{\sigma B_m^2}{\rho}\sin\gamma\ \cos\gamma\frac{\partial v}{\partial y}-\frac{\sigma B_m^2}{\rho}\sin^2\gamma\frac{\partial u}{\partial y}$$
$$-\frac{\sigma B_m^2}{\rho}\sin\gamma\ \cos\gamma\frac{\partial u}{\partial x}-\frac{\nu}{k^*}\frac{\partial u}{\partial y}. \tag{4.13}$$

The derivatives of above mentioned equation have been already calculated in Chapter 3.

$$\frac{\alpha^2 xyf'''}{4l^2(1-\alpha t)^3}+\frac{3\alpha^2 xf''}{4l(1-\alpha t)^{5/2}}+\frac{\alpha^2 xf'f''}{2l(1-\alpha t)^{5/2}}-\frac{\alpha^2 x}{4l(1-\alpha t)^{5/2}}(ff'''+f'f'')$$
$$=\frac{\alpha\nu xf^{(iv)}}{2l^3(1-\alpha t)^{5/2}}-\frac{\sigma B_0^2}{\rho}\sin\gamma\cos\gamma\frac{\alpha f'}{2(1-\alpha t)^2}-\frac{\sigma B_0^2}{\rho}\sin^2\gamma\frac{\alpha xf''}{2l(1-\alpha t)^{5/2}}$$
$$-\frac{\sigma B_0^2}{\rho}\sin\gamma\cos\gamma\frac{\alpha f'}{2(1-\alpha t)^2}-\frac{\nu}{k^*}\frac{\alpha xf''}{2l(1-\alpha t)^{3/2}}. \tag{4.14}$$

Multiply $\frac{2l^3(1-\alpha t)^{5/2}}{\alpha\nu x}$ on both sides, the dimensionless form of (4.14) can be reduced:

$$f^{(iv)}+\frac{l^2\alpha}{2\nu}(ff'''-3f''-f'f''-\eta f''')-\frac{\alpha\sigma l^2B_0^2}{\rho\nu}\ \sin\gamma\ (2\delta f'\cos\gamma+f''\ \sin\gamma)$$
$$-\frac{H^2}{k^*}f''=0,$$

$$f^{(iv)}+S(ff'''-3f''-f'f''-\eta f''')-M^2\ \sin\gamma\ (\sin\gamma f''+2\delta\cos\gamma f')$$
$$-\frac{1}{Da}f''=0. \tag{4.15}$$

Now we have to convert energy equation into ODE to utilize similarity transformation, in (4.10) T and v does not depend on x so the derivative of T and v is equal to zero,

$$T=\theta(\eta)(T_H-T_0)+T_0\quad;\quad v=v_Hf(\eta)\quad;\quad T_H=T_0+\frac{T_0}{1-\alpha t}$$
$$\frac{\partial T}{\partial x}\ =\ 0\qquad;\qquad\frac{\partial v}{\partial x}\ =\ 0.$$

$$\frac{\partial T}{\partial t}\ +\ v\ \frac{\partial T}{\partial y}\ =\ \frac{k}{\rho c_p}\ \frac{\partial^2 T}{\partial y^2}+\frac{\mu}{\rho c_p}\left[2\left(\frac{\partial u}{\partial x}\right)^2+2\left(\frac{\partial v}{\partial y}\right)^2+\left(\frac{\partial u}{\partial y}\right)^2\right]$$
$$+\frac{\sigma B_m^2}{\rho c_p}(u\sin\gamma-v\cos\gamma)^2+\frac{16\sigma^* T_H^3}{3k^*\rho c_p}\frac{\partial^2 T}{\partial y^2}. \tag{4.16}$$

The derivatives of above mentioned equation have been already calculated in Chapter 3.

$$\frac{\theta(\eta)\alpha T_0}{(1-\alpha t)^2} - \frac{\theta'(\eta)T_0 y H'(t)}{(1-\alpha t)H^2(t)} + \frac{v_H f(\eta)T_0\theta'(\eta)}{H(t)(1-\alpha t)} = \frac{k}{\rho c_p}\frac{T_0\theta''(\eta)}{H^2(t)(1-\alpha t)}$$
$$+ \frac{\nu}{c_p}\left(\frac{4v_H^2 f'^2(\eta)}{H^2} + \frac{x^2 v_H^2 f''^2(\eta)}{H^4}\right) + \frac{\sigma B_m^2}{\rho c_p}\left(\frac{-x v_H f'(\eta)}{H}\sin\gamma - v_H f(\eta)\cos\gamma\right)^2$$
$$+ \frac{16\sigma^* T_H^3}{3k^*\rho c_p}\frac{T_0\theta''(\eta)}{H^2(t)(1-\alpha t)}. \tag{4.17}$$

Multiplying $\frac{H^2(t)(1-\alpha t)\rho c_p}{kT_0}$ on both sides, the dimensionless form of (4.10) can be reduced:

$$\theta'' + SPr(f\theta' - \eta\theta' - 2\theta) + PrEc[f''^2 + 4\delta^2 f'^2 + M^2(f'^2 sin^2\gamma +$$
$$\delta^2 f^2\cos^2\gamma + 2\delta f f'\sin\gamma\cos\gamma)] + Rd\theta'' = 0.$$

$$(1+Rd)\theta'' + SPr(f\theta' - \eta\theta' - 2\theta) + PrEc[f''^2 + 4\delta^2 f'^2 + M^2(f'^2 sin^2\gamma +$$
$$\delta^2 f^2\cos^2\gamma + 2\delta f f'\ \sin\gamma\ \cos\gamma\ )]\ =\ 0. \tag{4.18}$$

The final dimensionless form of the governing model is

$$f^{(iv)} + S\ (ff''' - 3f'' - f'f'' - \eta f''') - M^2\ \sin\gamma\ (\sin\gamma\ f'' + 2\delta\cos\gamma\ f')$$
$$- \frac{1}{Da}f'' = 0. \tag{4.19}$$

$$(1+Rd)\theta'' + SPr(f\theta' - \eta\theta' - 2\theta) + PrEc[f''^2 + 4\delta^2 f'^2 + M^2(f'^2 sin^2\gamma +$$
$$\delta^2 f^2\cos^2\gamma + 2\delta f f'\ \sin\gamma\ \cos\gamma)] = 0. \tag{4.20}$$

The associated boundary conditions of (4.5) and (4.6) shown as:

$$f'(\eta) = R\,,\quad f(\eta) = S_b\,,\quad \theta(\eta) = 0,\quad \text{at}\quad \eta = 0, \tag{4.21}$$
$$f'(\eta) = 0\,,\quad f(\eta) = 1\,,\quad \theta(\eta) = 1,\quad \text{at}\quad \eta = 1. \tag{4.22}$$

Different parameters used in (4.19) and (4.20) are defined as follow:

$$\left.\begin{aligned} S=\frac{\alpha l^2}{2\nu},\quad Pr=\frac{\mu C_p}{k},\quad Ec=\frac{u_0^2}{C_pR^2(T_H-T_0)},\quad Da=\frac{k^*}{H^2},\\ M^2=\frac{\sigma B_0^2 l^2}{\rho\nu},\quad S_b=\frac{2v_0}{\alpha l},\quad R=\frac{u_s\delta}{v_H},\quad \delta=\frac{H}{x},\quad Rd=\frac{16\sigma^* T_H^3}{3k^*k}. \end{aligned}\right\} \tag{4.23}$$

4.2 Physical Quantities

The quantities of practical interest in this study are the Nusselt number (Nu) and the skin friction coefficient (C_f), respectively.
The skin friction coefficient C_f have been already derived in Chapter 3.

The Nusselt number coefficient Nu is characterized by:

$$Nu=\frac{l}{k(T_H-T_0)}\left(-k\frac{\partial T}{\partial y}_{y=H(t)}+q_r\right), \tag{4.24}$$

$$T=\theta(\eta)\left(\frac{T_0}{1-\alpha t}\right)+T_0$$

$$\frac{\partial T}{\partial y}=\left(\frac{T_0}{1-\alpha t}\right)\theta'(\eta)\frac{1}{l(1-\alpha t)^{1/2}}$$

$$\frac{\partial T}{\partial y}=\frac{T_0\theta'(\eta)}{l(1-\alpha t)^{3/2}}$$

$$Nu=\frac{l}{k(T_H-T_0)}\left(-k\frac{T_0\theta'(\eta)}{l(1-\alpha t)^{3/2}}-\frac{16\sigma^*T_H^3}{3k^*}\frac{\partial T}{\partial y}\right)$$

$$Nu=\frac{l}{k(T_H-T_0)}\left(-k\frac{T_0\theta'(\eta)}{l(1-\alpha t)^{3/2}}-\frac{16\sigma^*T_H^3}{3k^*}\frac{T_0\theta'(\eta)}{l(1-\alpha t)^{3/2}}\right)$$

$$Nu=-\frac{l}{k(T_H-T_0)}\frac{kT_0\theta'(\eta)}{l(1-\alpha t)^{3/2}}\left(1+\frac{16\sigma^*T_H^3}{3k^*k}\right)$$

$$Nu=-\frac{1}{T_H-T_0}\left(\frac{T_0\theta'(\eta)}{(1-\alpha t)^{3/2}}\right)\left(1+\frac{16\sigma^*T_H^3}{3k^*k}\right)\because\left(T_H-T_0=\frac{T_0}{1-\alpha t}\right)$$

$$Nu=-\frac{(1-\alpha t)}{T_0}\left(\frac{T_0\theta'(\eta)}{(1-\alpha t)^{3/2}}\right)\left(1+\frac{16\sigma^*T_H^3}{3k^*k}\right)$$

$$Nu=-\frac{\theta'(\ \eta\ )}{(\ 1\ -\ \alpha\ t)^{\ 1/2}}(1+Rd)$$

$$-(1+Rd)\theta'(\ \eta\ )=Nu\left((1-\alpha t)^{1/2}\right)$$

$$-(1+Rd)\theta'(\eta)=Nu\left(\frac{(1-\alpha t)^{1/2}}{(bx)^{\ 1/2}}(bx)^{1/2}\right)$$

$$
\begin{aligned}
-(1+Rd)\theta'(\eta) &= Nu\left(\frac{(bx)^{1/2}}{(u_s)^{1/2}}\right) \qquad \because \left(u_s = \frac{bx}{1-\alpha t}\right)\\
-(1+Rd)\theta'(\eta) &= Nu\left(\frac{b^{1/2}x}{(u_s x)^{1/2}}\right)\\
-(1+Rd)\theta'(\eta) &= Nub^{1/2}x\frac{\nu^{1/2}}{(u_s x)^{1/2}}\frac{1}{\nu^{1/2}}\\
-(1+Rd)\theta'(\eta) &= \frac{Nub^{1/2}x}{\nu^{1/2}}\frac{1}{(Re_x)^{1/2}}\\
-(1+Rd)\theta'(\eta) &= \left(\frac{\nu}{b}\right)^{-1/2}x(Re_x)^{-1/2}Nu \quad at \quad \eta = 1,
\end{aligned} \tag{4.25}
$$

where $Re_x = \frac{u_s x}{\nu}$ represent the local Reynolds number.

4.3 Numerical Solution

For the solution of ODEs, (4.19) and (4.20), the shooting method has been used. The missing ICs $f''(0)$, $f'''(0)$ and $\theta'(0)$ are denoted by χ_1, χ_2 and χ. For further refining of the missing conditions, Newton's method will be used. Furthermore, the following notations have been used.

$$
\begin{aligned}
&\Rightarrow \quad f = f_1\,, \quad f' = f_2\,, \quad f'' = f_3\,, \quad f''' = f_4\,, \quad f^{(iv)} = f_4'\\
&\frac{\partial f_1}{\partial \chi_1} = f_5, \quad \frac{\partial f_2}{\partial \chi_1} = f_6, \quad \frac{\partial f_3}{\partial \chi_1} = f_7, \quad \frac{\partial f_4}{\partial \chi_1} = f_8\\
&\frac{\partial f_1}{\partial \chi_2} = f_9, \quad \frac{\partial f_2}{\partial \chi_2} = f_{10}, \quad \frac{\partial f_3}{\partial \chi_2} = f_{11}, \quad \frac{\partial f_4}{\partial \chi_2} = f_{12}.\\
&\Rightarrow \quad \theta = Y_1, \quad \theta' = Y_2, \quad \theta'' = Y_2'\\
&\frac{\partial Y_1}{\partial \chi} = Y_3, \quad \frac{\partial Y_2}{\partial \chi} = Y_4.
\end{aligned}
$$

The above mathematical problem model (4.19) and (4.20), can now be given as first order ODEs in the following form.

$$
\begin{aligned}
f_1' &= f_2 & f_1(0) &= 0.1,\\
f_2' &= f_3 & f_2(0) &= 0.5,\\
f_3' &= f_4 & f_3(0) &= \chi_1,
\end{aligned}
$$

$$
\begin{aligned}
f_4^{'} &= S(\eta f_4 + 3f_3 + f_2 f_3 - f_1 f_4) + M^2 \sin\gamma(\sin\gamma f_3 + 2\delta\cos\gamma f_2) \\
&\quad + \frac{1}{Da} f_3 && f_4\ (0) = \chi_2, \\
f_5^{'} &= f_6 && f_5\ (0) = 0, \\
f_6^{'} &= f_7 && f_6\ (0) = 0, \\
f_7^{'} &= f_8 && f_7\ (0) = 1, \\
f_8^{'} &= S(\eta f_8 + 3f_7 + f_2 f_7 + f_3 f_6 - f_1 f_8 - f_4 f_5) \\
&\quad + M^2\ \sin\gamma\ (\ f_7 \sin\gamma + 2\delta\ f_6 \cos\gamma) + \frac{1}{Da} f_7 && f_8\ (0) = 0, \\
f_9^{'} &= f_{10} && f_9\ (0) = 0, \\
f_{10}^{'} &= f_{11} && f_{10}\ (0) = 0, \\
f_{11}^{'} &= f_{12} && f_{11}\ (0) = 0, \\
f_{12}^{'} &= S(\eta f_{12} + 3f_{11} + f_2 f_{11} + f_{10} f_3 - f_1 f_{12} - f_4 f_9) \\
&\quad + M^2\ \sin\gamma\ (\ f_{11} \sin\gamma + 2\delta\ f_{10} \cos\gamma) + \frac{1}{Da} f_{11} && f_{12}\ (0) = 1, \\
Y_1^{'} &= Y_2 && Y_1\ (0) = 0, \\
Y_2^{'} &= \frac{1}{(1+Rd)}[-PrS(fY_2 - \eta Y_2 - 2Y_1) - PrEc[f^{''2} + 4\delta^2 f^{'2} \\
&\quad + M^2\ (f^{'2}\ \sin^2\gamma\ +\ f^2\delta^2\cos^2\gamma + 2ff^{'}\delta\ \sin\gamma\ \cos\gamma)]] && Y_2\ (0) = \chi, \\
Y_3^{'} &= Y_4 && Y_3\ (0) = 0, \\
Y_4^{'} &= \frac{1}{(1+Rd)}[-PrS(fY_4 - \eta Y_4 - 2Y_3)] && Y_4\ (0) = 1,
\end{aligned}
$$

The above IVP is numerically solved by RK4 method. To obtain the approximate solution, the problem domain was taken as [0 , 1]. In the above system of equations, the missing conditions χ_1, χ_2, and χ are to be chosen such that

$$f_1(1\ ,\ \chi_1\ ,\ \chi_2)\ =\ 0, \quad f_2(1\ ,\ \chi_1\ ,\ \chi_2) = 0, \quad Y_1(1\ ,\ \chi) = 0 \tag{4.26}$$

Newton's approach was applied to carry out the following iterative scheme for the refinement of the missing conditions:

$$\begin{bmatrix} \chi_1^{(n\ +\ 1)} \\ \chi_2^{(n\ +\ 1)} \end{bmatrix} = \begin{bmatrix} \chi_1^{(\ n\ )} \\ \chi_2^{(\ n\ )} \end{bmatrix} - \begin{bmatrix} f_5 & f_9 \\ f_6 & f_{10} \end{bmatrix}^{-1} \begin{bmatrix} f_1^{(\ n\ )} \\ f_2^{(\ n\ )} \end{bmatrix}_{(\chi_1^{(n)}, \chi_2^{(n)}, 1)}$$

and

$$\chi_{n+1} = \chi_n - \frac{Y_1(1,\chi) - 1}{Y_3(1,\chi)}, \tag{4.27}$$

1. Choice of the guesses $\chi_1 = \chi_1^{(0)}$, $\chi_2 = \chi_2^{(0)}$, and $\chi = \chi^{(0)}$.

2. Choosing a small positive number ϵ.
   If $max\{|f_1(1,\ \chi_1,\ \chi_2) - 1|, |f_2(1,\ \chi_1,\ \chi_2)\ -\ 0|\} < \epsilon$, stop the process otherwise go to (3).

3. Calculating ${\chi_1}^{(n\ +\ 1)}$ and ${\chi_2}^{(n\ +\ 1)}$, $\quad n = 0, 1, 2, 3...$ by using Newton scheme.
   If $max|Y_1(1,\ \chi) - 1| < \epsilon$, stop the process otherwise go to (4).

4. Compute $\chi^{\ (n\ +\ 1)}$, $n = 0, 1, 2, 3...$ by using Newton scheme.
   where $\epsilon = 10^{-10}$ is the tolerance for the modeled problem.

4.4 Graphical Results

In order to show the squeezing movement more accurately, the computed results are presented and discussed graphically. Figures 4.1-4.14 shows the variations in velocity and temperature curves against some of the parameters including squeeze parameter S, the angle of magnetic inclination γ, the magnetic parameter M, the lower plate stretching parameter, Eckert number Ec, the lower plate suction/injection parameter, Da is the darcy number and Rd is the radiation parameter.

Figure 4.1 and 4.2 indicate the squeeze number effect on velocity and temperature. Figure 4.1 demonstrates the distribution of fluid velocity in regions near the lower or upper end of plates are decreasing due to rising of the squeeze number, but for the velocity an opposite effect has been observed close to the centre between the plates. It is noted from Figure 4.2 that increasing value of the squeezing number causes reduction in the temperature. When the plates move close to each other,

the temperature field will be comparatively high.

Figure 4.3 and 4.4 represent the fluid velocity and temperature for various values of the magnetic number. It has been observed in Figure 4.3 that an increase in the magnetic parameter causes the fluid velocity to increase at both ends (lower and upper) of the plates, but the fluid velocity near the center, quite slightly, shows a noticeable decrease. The fluid in the central regions has larger Lorentz force than the fluid near the plate. The reason is that the Lorentz force in fluid motion presents resistance. So excessive Lorentz forces make velocity slow down close the central region of plates. Figure 4.4 shows that the fluid temperature rises from the lower plate to the upper plate surface when the magnetic field parameter rises. For the larger magnetic value, the fluid temperature increases not only near the upper surface but also in the centre between the plates. Actually, the strong magnetic field affects the temperature distribution in the regions. Large friction along with a strong magnetic field generates more heat in fluids.

Velocity and temperature profiles variations were shown through Figures 4.5 and 4.6 by rising value of the magnetic angle. The angle of magnetic inclination ranges between 0 and $\pi/2$. Similar profiles behaviors of velocity and temperature were obtained from both figures when compared to the corresponding profiles of different magnetic parameter values. The angle of magnetic field inclination γ effects on both the fluid velocity and the temperature are similar to those of the magnetic parameter. Therefore, the transfer of fluid in the squeezing movement in practical applications related to momentum and heat control, the affects generated by changing the strength of the magnetic field can also be obtained by modifying the angle of magnetic field inclination.

Figures 4.7 and 4.8 show the impact of stretching parameter of the lower plate on the velocity and temperature. In Figure 4.7 the fluid velocity increases close to the lower plate as compared to the fluid velocity close to the upper plate. Furthermore,

as the stretching parameter on the lower surface rises slowly, the maximum value of velocity can be seen in the surface of lower plate. Figure 4.8 reflects that when we rise the stretching parameter of the lower plate, the fluid temperature above the lower plate decreases and increases thereafter, when we take the stretching parameter $R > 1.5$ the fluid temperature close to the upper plate at first increases and then steadily decreases.

Figure 4.9 and 4.10 represent the effects of lower-plate suction/injection parameter on the fluid velocity and temperature profiles. Figure 4.9 indicates a decline in velocity for the lower plate suction/injection parameter. In addition, as the lower plate stretches for greater suction across the lower plate, the maximum fluid velocity does not show in the centre between the plates, and subsequently fluid velocity reduces from the lower to upper surface of the plate. In order to increase the suction/injection parameter, the temperature profiles decrease. In particular, it was noted that as the suction/injection parameter S_b reduces, the maximum fluid temperature does not occur on the upper surface of the plate but in the centre between the two plates.

The temperature for different values of Eckert number was shown in Figure 4.11. A clear temperature rise is observed to increase the values of Eckert number. This increase in the thermal field is evident because Eckert has directly affects on the process of heat dissipation, which in turn increases the temperature field between the plates. Figure 4.11 also indicates that the maximum fluid temperature occurs in the centre between the two plates for larger Eckert number, whereas it tends to be smaller in the upper plate.

Figure 4.12 shows the characteristics of the velocity profile corresponding to the inverse Darcy number. It indicates that an increase in the Darcy number causes the fluid velocity to decrease at both ends (lower and upper) of the plates, but the fluid velocity near the center shows a noticeable increase. Higher values of

the inverse Darcy number lead to a greater resistance to flow. It has been show in Figure 4.13 that the fluid temperature rises from lower surface of the plate to the upper surface of the plate when the Darcy number is small. For the larger Darcy number, the fluid temperature rise not only on the above surface but also on centre between two plates.

Figure 4.14 shows the radiation parameter influence on the temperature profile distribution. It is observed that the temperature profile decreases substantially by increasing the radiation parameter. This is because the increasing radiation parameter values contribute to a reduction in the thickness of the boundary layer and to an increase in the heat transfer rate with chemical impact on the melting surface.

Figures 4.15 and 4.16 demonstrate the effects of the squeeze parameter and magnetic angle on the coefficient of skin friction and the Nusselt number, where the magnetic inclination angle ranges among 0^0 to 90^0. The absolute value of skin friction and Nusselt number may be noticed as a decreasing function of the angle of magnetic inclination γ. In addition, for the increment of squeeze parameter and the angle of magnetic inclination are fixed, then the Nusselt number increases and skin friction coefficient decreases.

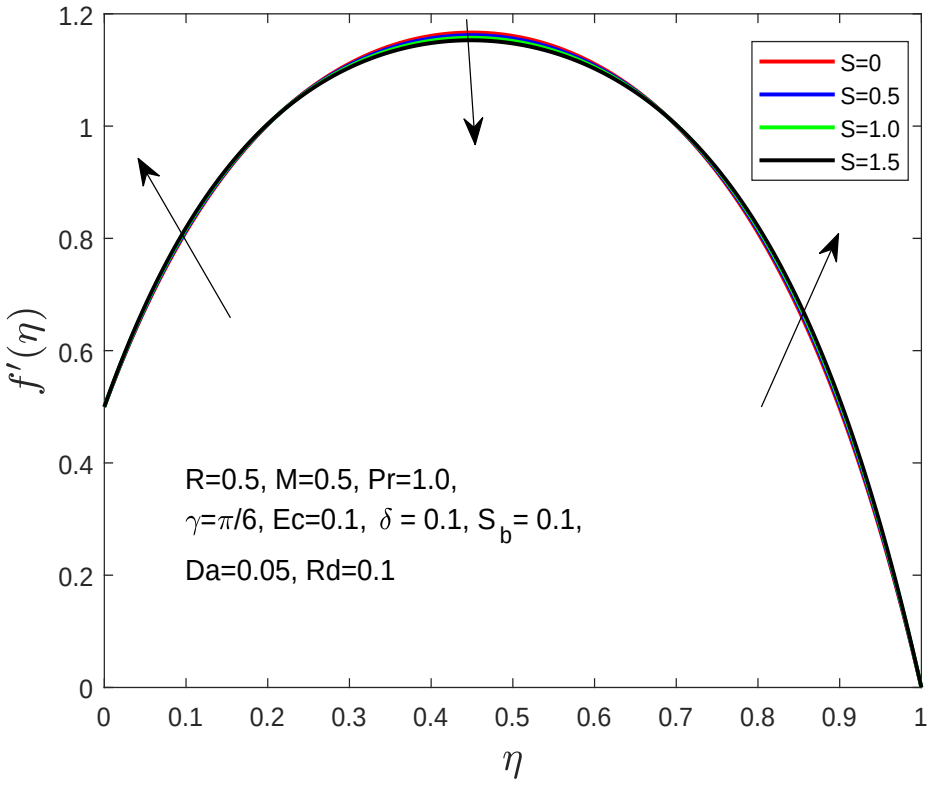

Figure 4.1: Effect of S on the f'.

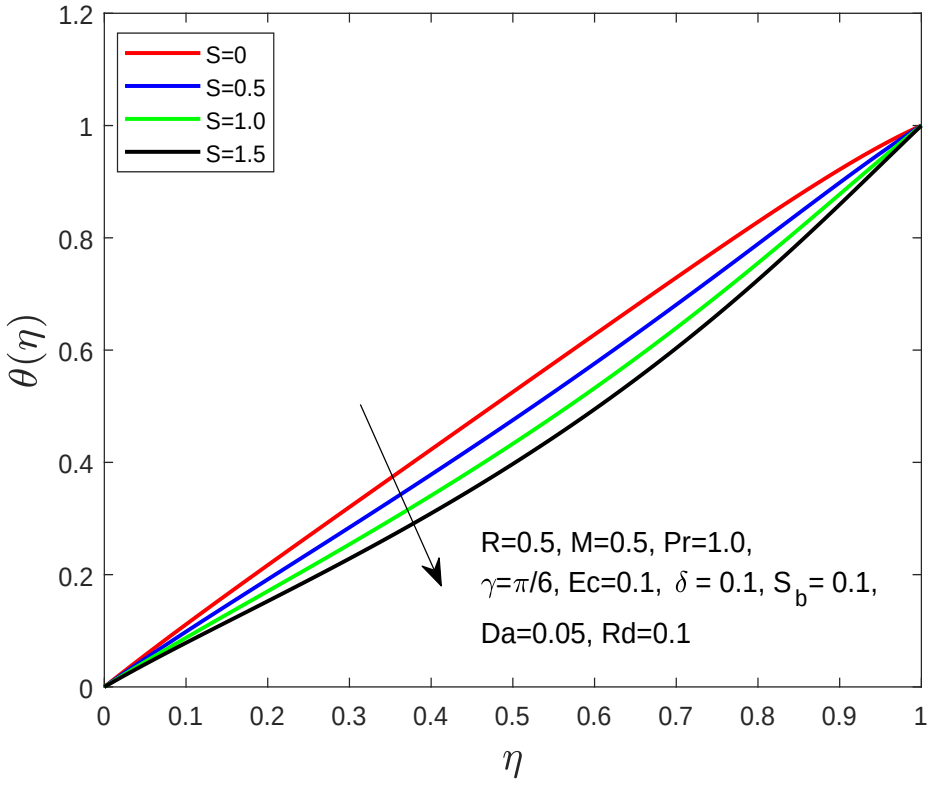

Figure 4.2: Effect of S on the $\theta(\eta)$.

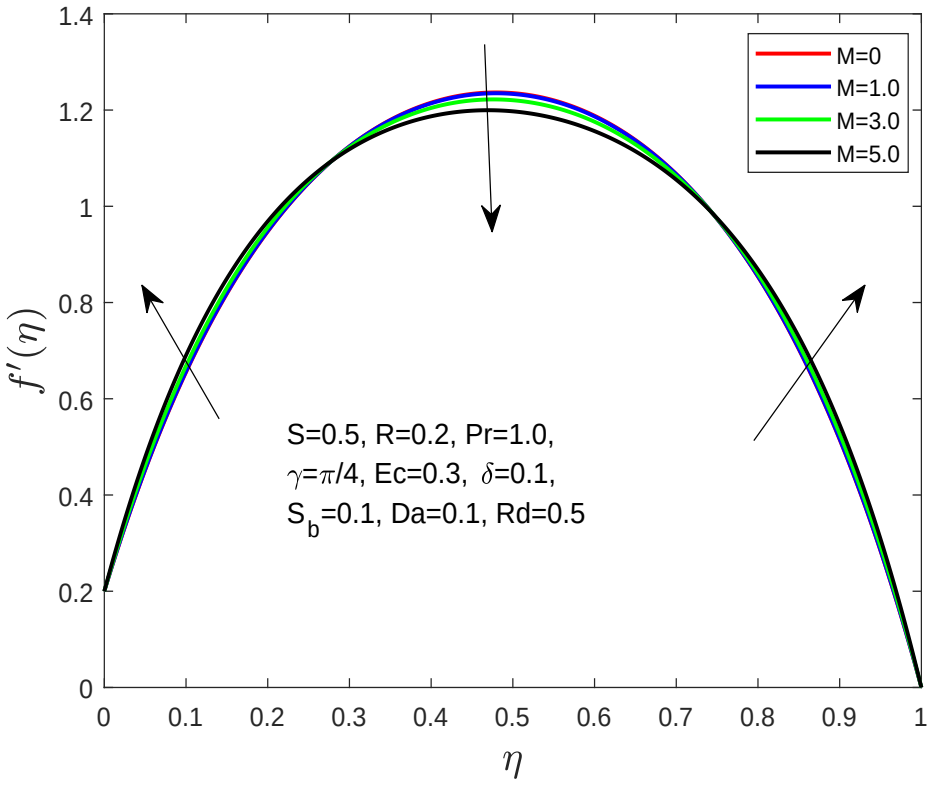

Figure 4.3: Effect of M on the f'.

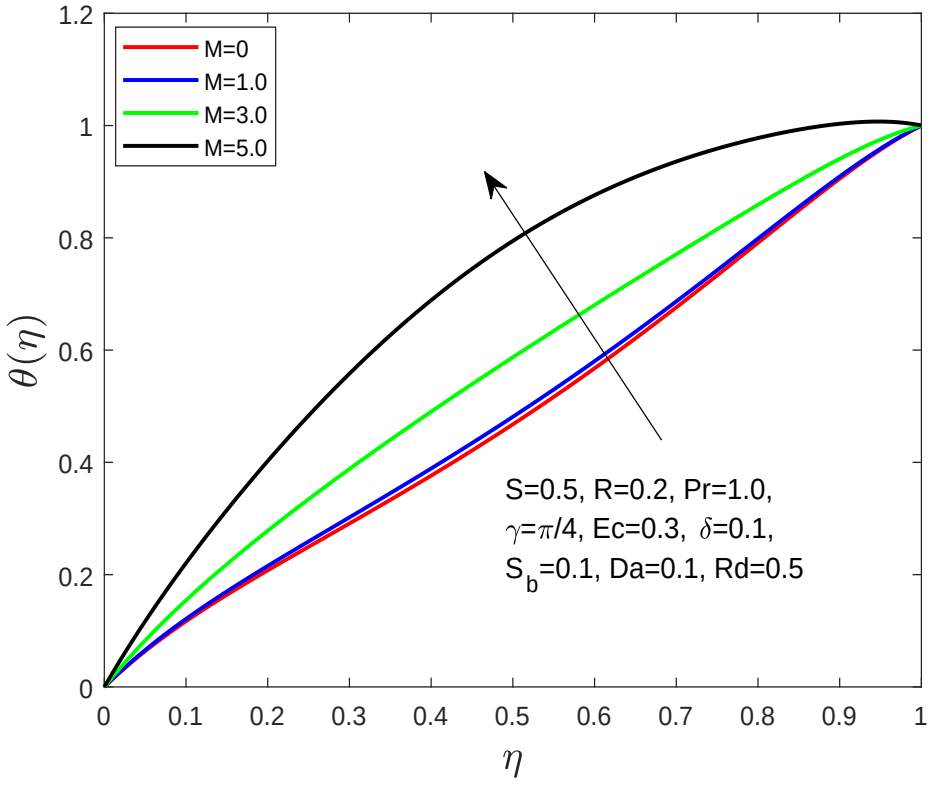

Figure 4.4: Effect of M on the $\theta(\eta)$.

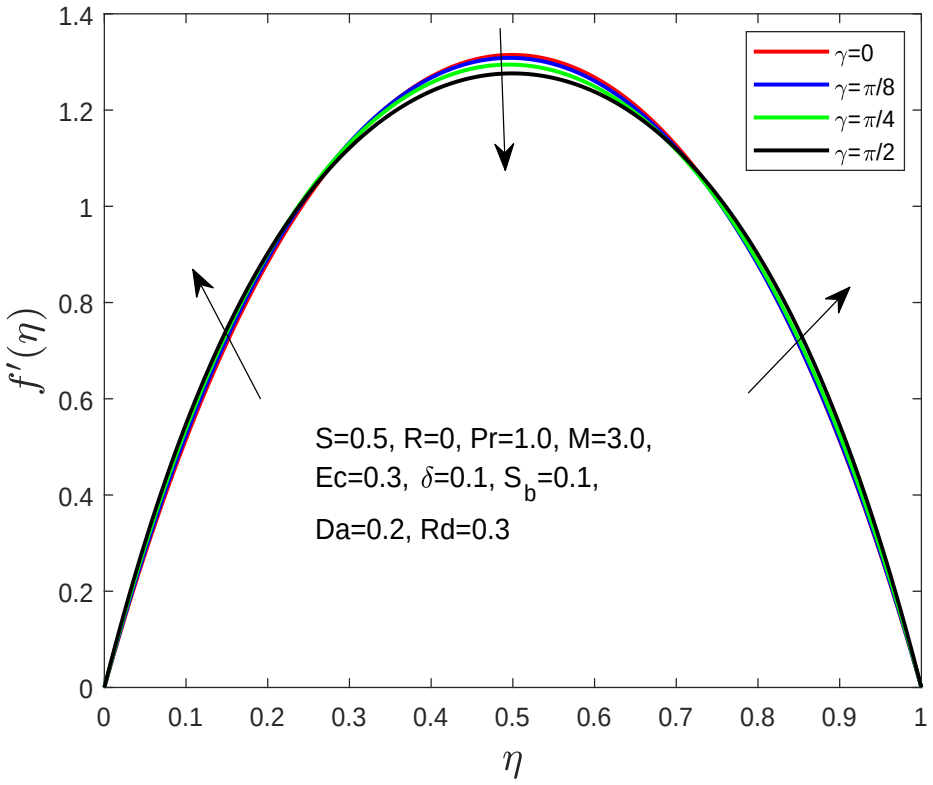

Figure 4.5: Effect of γ on the f'.

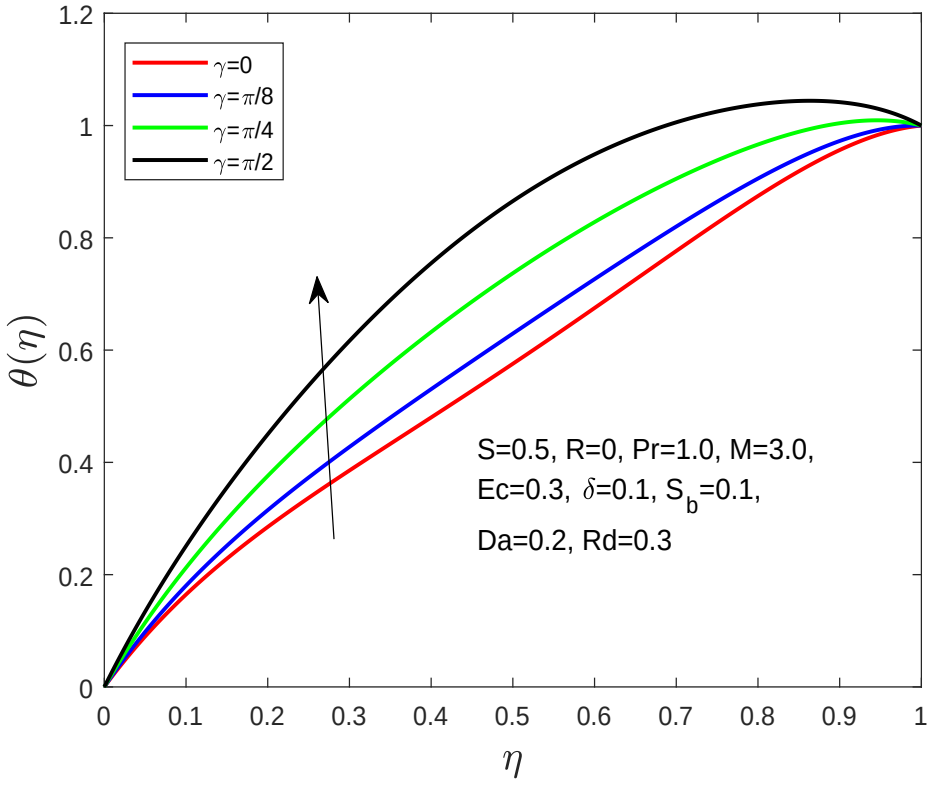

Figure 4.6: Effect of γ on the $\theta(\eta)$.

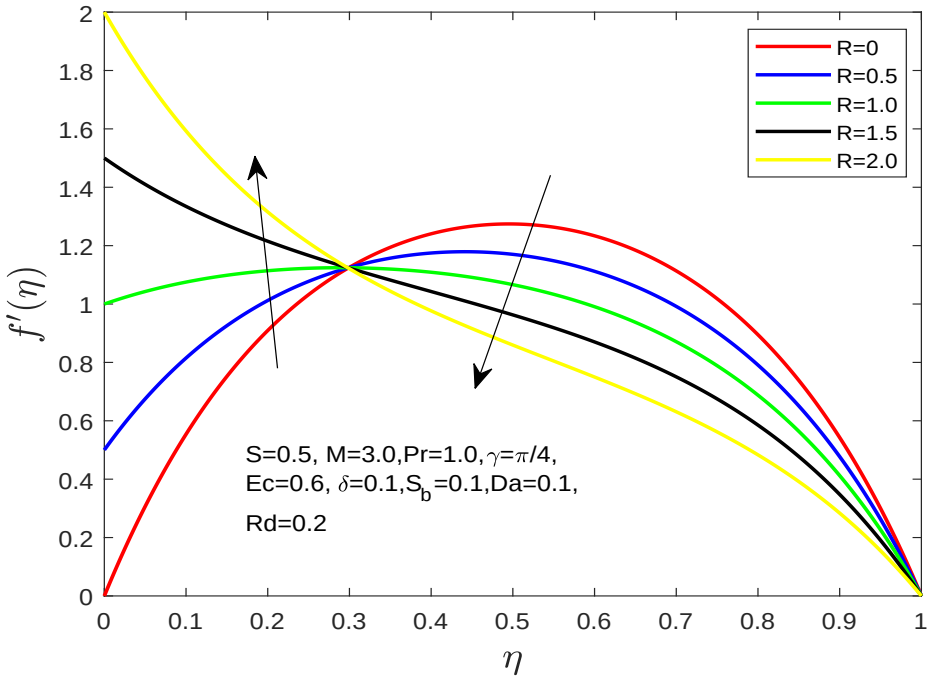

Figure 4.7: Effect of R on the f'.

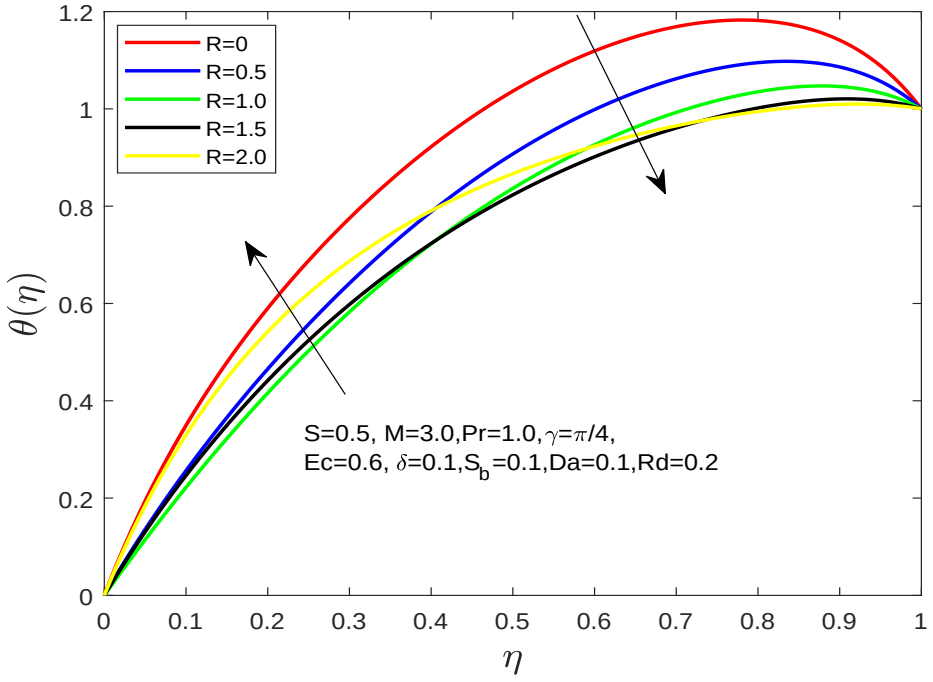

Figure 4.8: Effect of R on the $\theta(\eta)$.

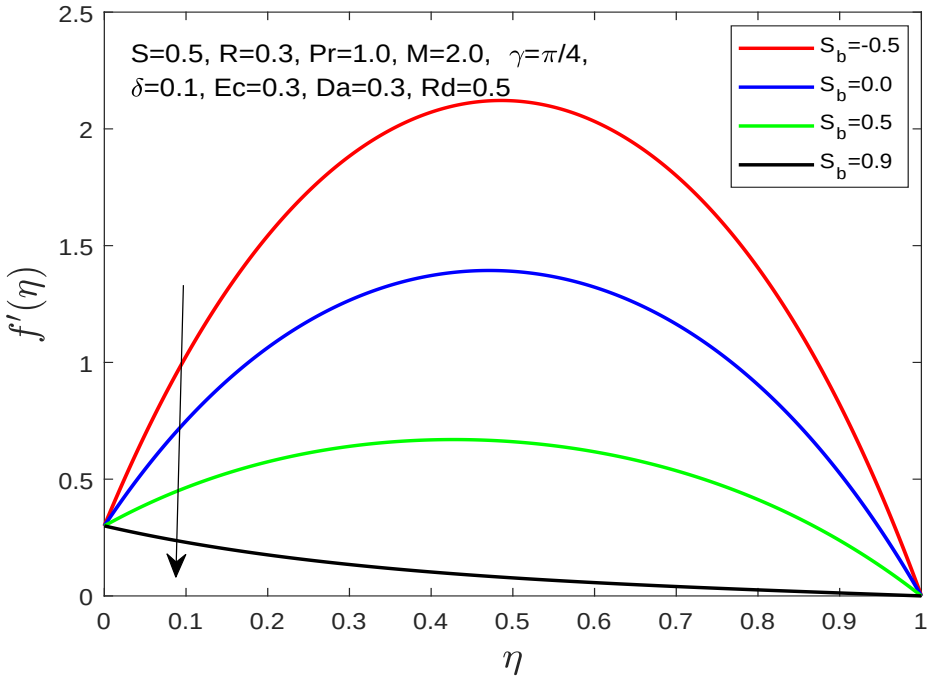

Figure 4.9: Effect of S_b on the f'.

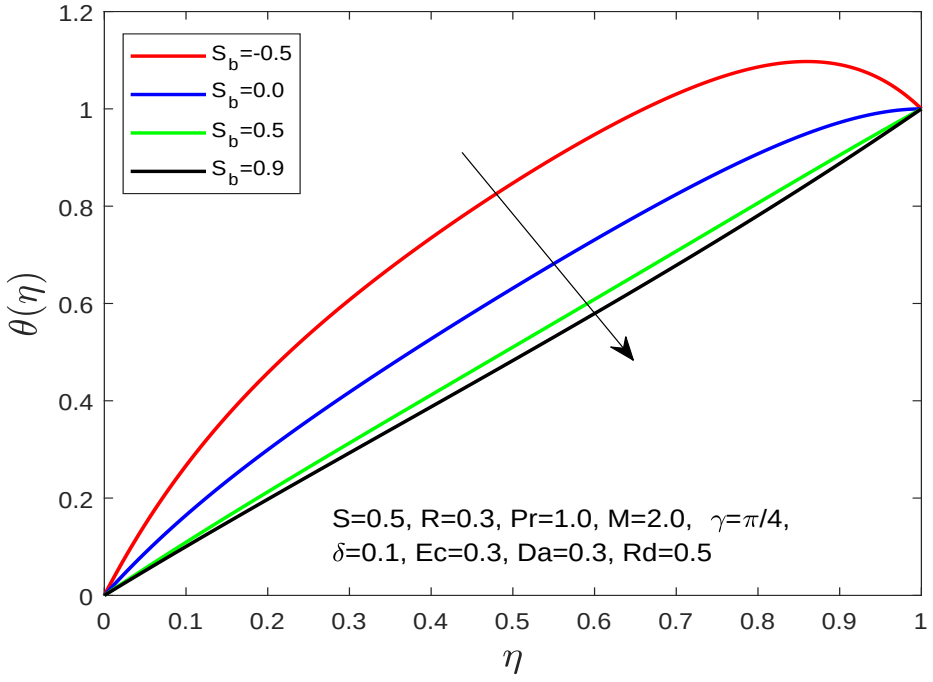

Figure 4.10: Effect of S_b on the $\theta(\eta)$.

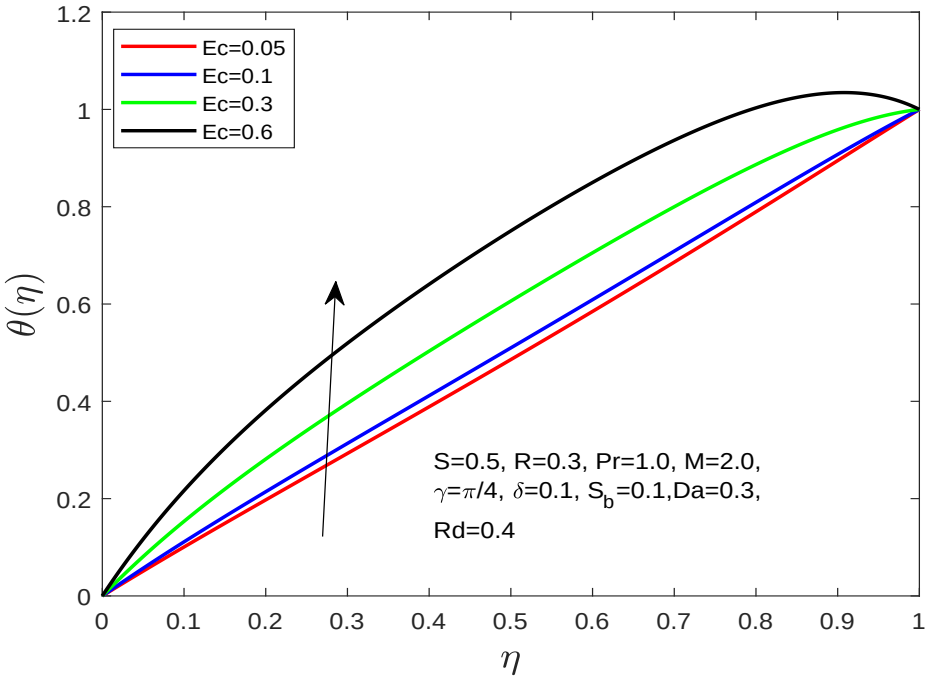

Figure 4.11: Effect of Ec on the $\theta(\eta)$.

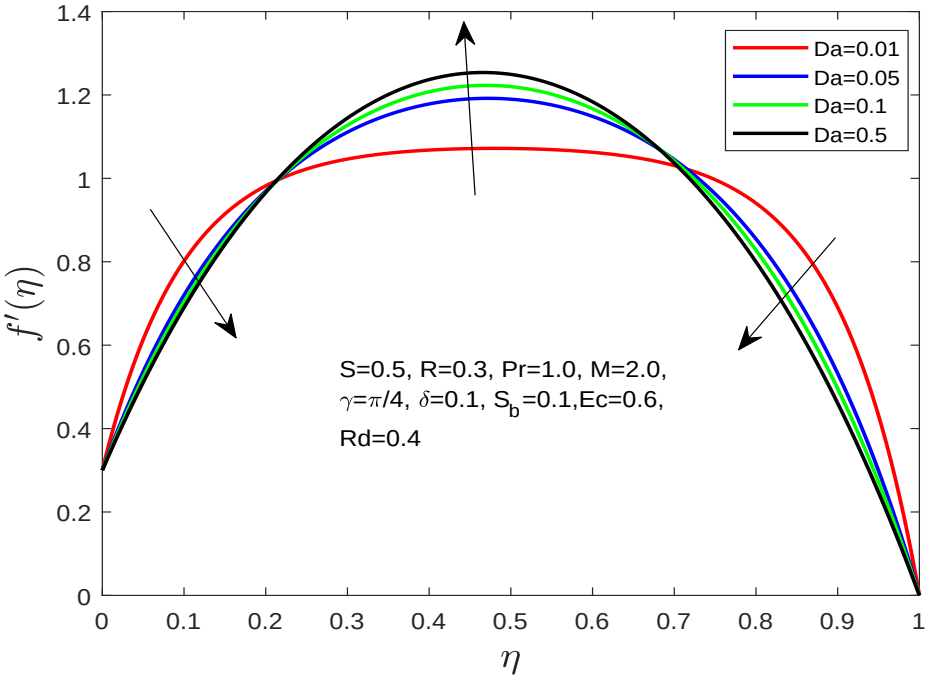

Figure 4.12: Effect of Da on the f'.

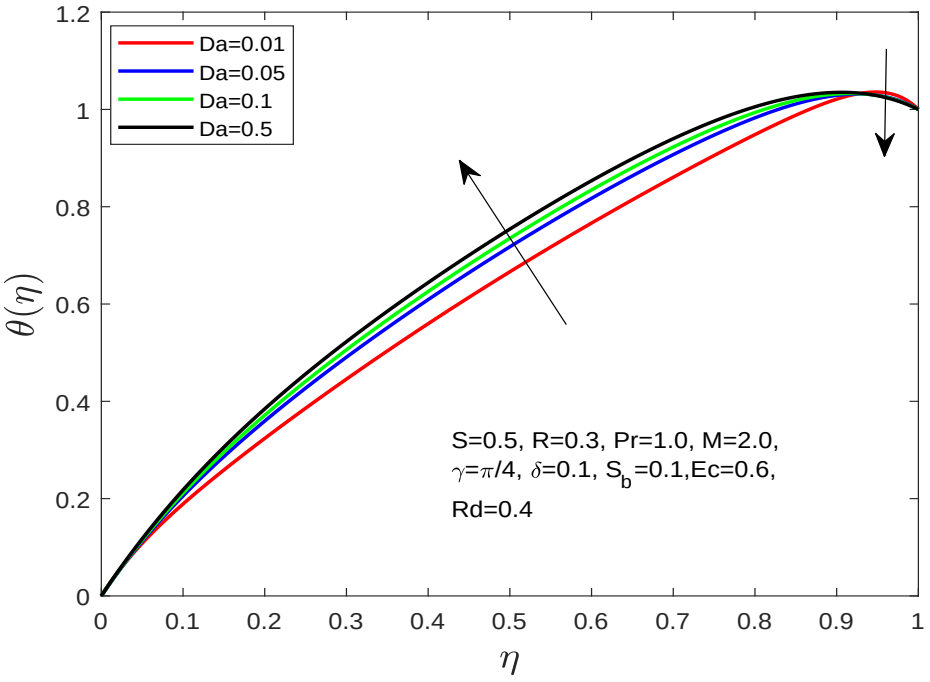

Figure 4.13: Effect of Da on the $\theta(\eta)$.

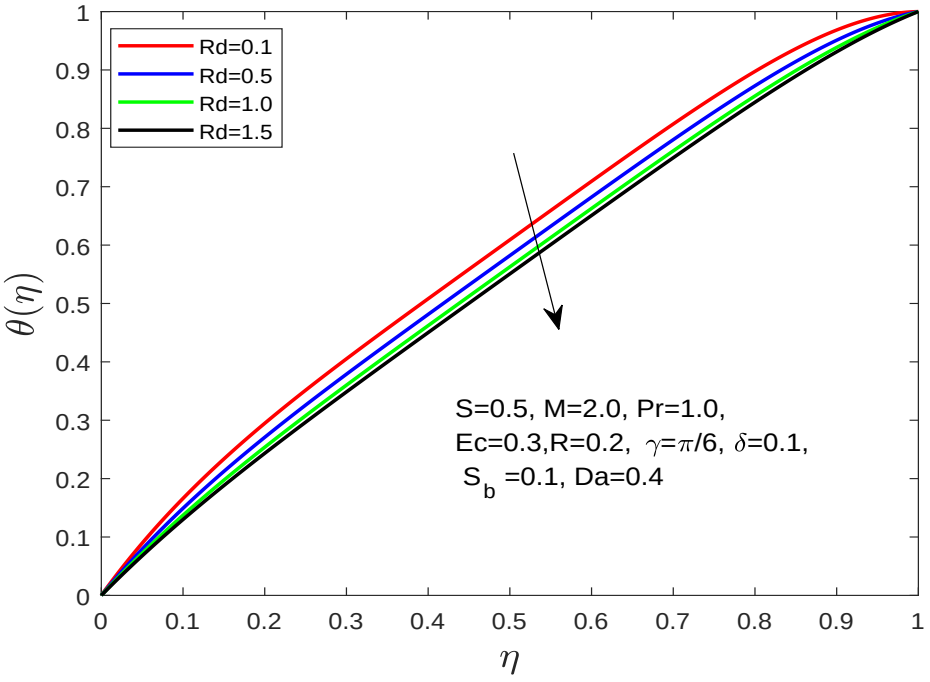

Figure 4.14: Effect of Rd on the $\theta(\eta)$.

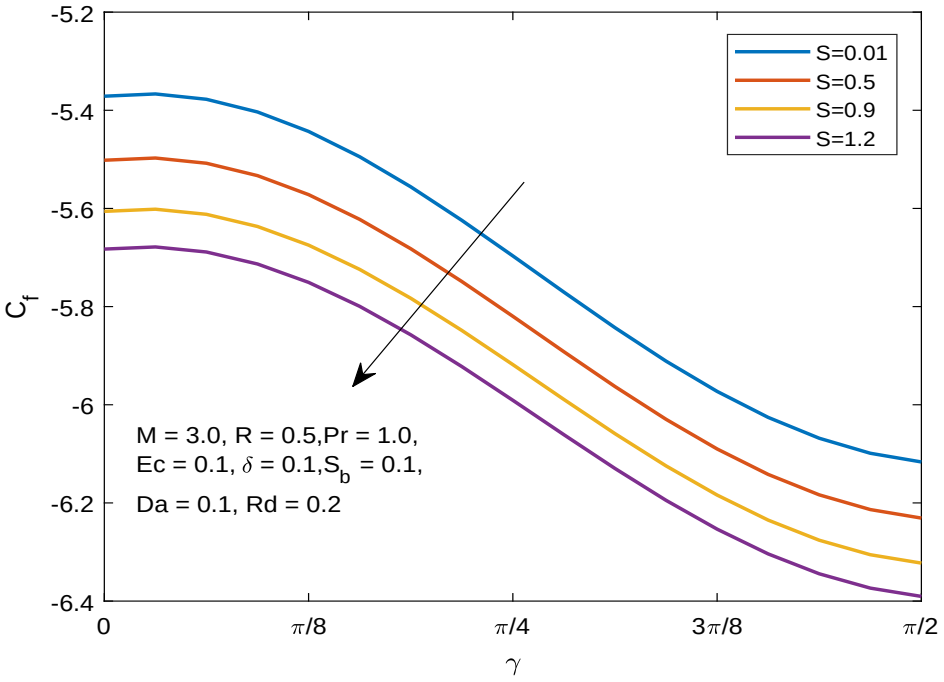

Figure 4.15: Effect of S and γ on the C_f.

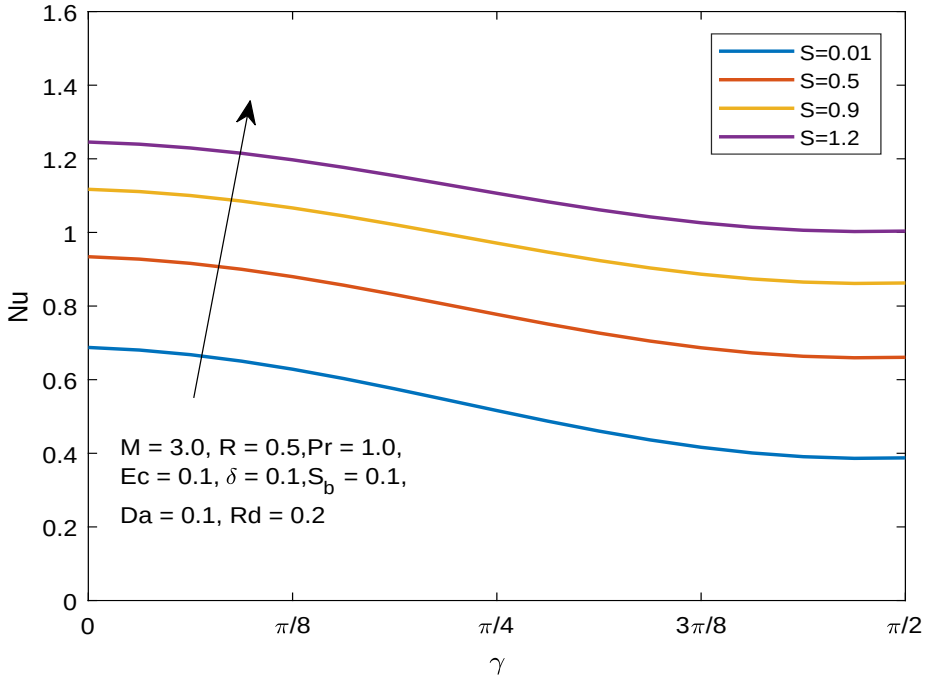

Figure 4.16: Effect of S and γ on Nu.

Chapter 5

Conclusion

Summary of this research work represents the analysis of squeezing movement of viscous fluid past between two infinite parallel plates considered along stretching surface in a porous medium with the influence of magnetic field. By utilizing similarity transformation we reduced the set of nonlinear PDEs into a set of nonlinear ODEs and then solved numerically. Numerical results are obtained for the set of nonlinear ODEs by using the well known shooting technique with Runge-Kutta method of order four (RK4). Significance of the effect of different physical parameters under discussion on the dimensionless velocity and temperature are describe graphically. The skin friction and the Nusselt number for different value of the distinctive governing parameters are also presented graphically. After a detailed examination, we arrived at the following conclusion.

- Increasing the value of Squeeze parameter (S), the velocity close to the lower or upper end of plates is increasing, but for the velocity profile decreasing between the centre of the plates and the temperature profile tends to decrease.
- The magnetic field (M) has a direct relation with the temperature profile and an inverse with the velocity profile.
- Increasing the angle of magnetic inclination (γ), the velocity close to the lower or upper end of plates is decreasing, but for the velocity profile an

opposite effect has been observed close to the centre between the plates and the temperature profile tends to increase.

- The lower plate suction/injection parameter (S_b) has an inverse relation with the velocity and temperature profile.

- Increase value of the Eckert number (Ec), the temperature profile tends to increase.

- Increase in the Darcy number (Da) causes the fluid velocity to decrease at both ends (lower and upper) of the plates, but the fluid velocity near the center shows a noticeable increase and the temperature profile begins to increase.

- Increase value of the thermal radiation (Rd), the temperature profile begins to decline.

- For the increment of Squeeze parameter (S) and the angle of magnetic inclination (γ), the skin friction (C_f) decreases and the Nusselt number (Nu) increases.

Bibliography

[1] G. B. Meir, *Basic of fluid mechanics*, vol. 1. Potto Project NFP, 2013.

[2] M. J. Stefan, "Versuch über die scheinbare adhesion," *Akademie der Wissenschaften in Wien. Mathematik-Naturwissen*, vol. 230, no. 69, pp. 713–721, 1874.

[3] J. Jackson, "A study of squeezing flow," *Applied Scientific Research, Section A*, vol. 11, no. 1, pp. 148–152, 1963.

[4] R. Usha and R. Sridharan, "Arbitrary squeezing of a viscous fluid between elliptic plates," *Fluid Dynamics Research*, vol. 18, no. 1, pp. 35–51, 1996.

[5] O. Reynolds, "IV. On the theory of lubrication and its application to Mr. Beauchamp towers experiments, including an experimental determination of the viscosity of olive oil," *Philosophical transactions of the Royal Society of London*, no. 177, pp. 157–234, 1886.

[6] F. Archibald, "Load capacity and time relations for squeeze films," *Transactions of the American Society of Mechanical Engineers*, vol. 78, pp. A231–A245, 1965.

[7] M. Mahmood, S. Asghar, and M. Hossain, "Squeezed flow and heat transfer over a porous surface for viscous fluid," *International Journal of Heat and mass Transfer*, vol. 44, no. 2, pp. 165–173, 2007.

[8] T. Hayat, M. Khan, M. Imtiaz, and A. Alsaedi, "Squeezing flow past a riga plate with chemical reaction and convective conditions," *Journal of Molecular Liquids*, vol. 225, pp. 569–576, 2017.

[9] M. Mustafa, T. Hayat, and S. Obaidat, "On heat and mass transfer in the unsteady squeezing flow between parallel plates," *Meccanica*, vol. 47, no. 7, pp. 1581–1589, 2012.

[10] S. Ahmad, M. Farooq, M. Javed, and A. Anjum, "Slip analysis of squeezing flow using doubly stratified fluid," *Results in Physics*, vol. 9, pp. 527–533, 2018.

[11] T. Hayat and S. Hina, "Effects of heat and mass transfer on peristaltic flow of williamson fluid in a non-uniform channel with slip conditions," *International Journal for numerical methods in fluids*, vol. 67, no. 11, pp. 1590–1604, 2011.

[12] S. Ahmad, M. Farooq, M. Javed, and A. Anjum, "Double stratification effects in chemically reactive squeezed sutterby fluid flow with thermal radiation and mixed convection," *Results in physics*, vol. 8, pp. 1250–1259, 2018.

[13] A. Khaled and K. Vafai, "Hydromagnetic squeezed flow and heat transfer over a sensor surface," *International Journal of Engineering Science*, vol. 42, no. 5-6, pp. 509–519, 2004.

[14] D. Ganji, M. Abbasi, J. Rahimi, M. Gholami, and I. Rahimipetroudi, "On the MHD squeeze flow between two parallel disks with suction or injection via Homotopy Analysis Method and Homotopy Perturbation Method," *Frontiers of Mechanical Engineering*, vol. 9, no. 3, pp. 270–280, 2014.

[15] S. Islam, H. Khan, I. A. Shah, and G. Zaman, "An axisymmetric squeezing fluid flow between the two infinite parallel plates in a porous medium channel," *Mathematical Problems in Engineering*, vol. 2011, 2011.

[16] H. Kandasamy, Ramasamy and Ishak, "Effect of chemical reaction, heat and mass transfer on nonlinear boundary layer past a porous shrinking sheet in the presence of suction," *Nuclear Engineering and Design*, vol. 240, no. 5, pp. 933–939, 2010.

[17] N. Acharya, K. Das, and P. K. Kundu, "The squeezing flow of Cu-water and Cu-kerosene nanofluids between two parallel plates," *Alexandria Engineering Journal*, vol. 55, no. 2, pp. 1177–1186, 2016.

[18] M. Fakour, A. Vahabzadeh, D. Ganji, and M. Hatami, "Analytical study of micropolar fluid flow and heat transfer in a channel with permeable walls," *Journal of Molecular Liquids*, vol. 204, pp. 198–204, 2015.

[19] A. M. Siddiqui, S. Irum, and A. R. Ansari, "Unsteady squeezing flow of a viscous MHD fluid between parallel plates, a solution using the Homotopy Perturbation Method," *Mathematical Modelling and Analysis*, vol. 13, no. 4, pp. 565–576, 2008.

[20] W. Tan and T. Masuoka, "Stokes first problem for a second grade fluid in a porous half-space with heated boundary," *International Journal of Non-Linear Mechanics*, vol. 40, no. 4, pp. 515–522, 2005.

[21] M. Wahiduzzaman, M. S. Khan, and I. Karim, "MHD convective stagnation flow of nanofluid over a shrinking surface with thermal radiation, heat generation and chemical reaction," *Procedia Engineering*, vol. 105, pp. 398–405, 2015.

[22] M. Sheikholeslami and D. Ganji, "Nanofluid hydrothermal behavior in existence of Lorentz forces considering Joule heating effect," *Journal of Molecular Liquids*, vol. 224, pp. 526–537, 2016.

[23] M. Sheikholeslami, D. Ganji, and M. Rashidi, "Magnetic field effect on unsteady nanofluid flow and heat transfer using Buongiorno model," *Journal of Magnetism and Magnetic Materials*, vol. 416, pp. 164–173, 2016.

[24] N. Rudraswamy, B. Gireesha, and M. Krishnamurthy, "Effect of internal heat generation/absorption and viscous dissipation on MHD flow and heat transfer of nanofluid with particle suspension over a stretching surface," *Journal of Nanofluids*, vol. 5, no. 6, pp. 1000–1010, 2016.

[25] M. Sheikholeslami and A. J. Chamkha, "Influence of Lorentz forces on nanofluid forced convection considering Marangoni convection," *Journal of Molecular Liquids*, vol. 225, pp. 750–757, 2017.

[26] M. Sheikholeslami, M. Rashidi, and D. Ganji, "Effect of non-uniform magnetic field on forced convection heat transfer of Fe_3O_4–water nanofluid," *Computer Methods in Applied Mechanics and Engineering*, vol. 294, pp. 299–312, 2015.

[27] M. Sheikholeslami, K. Vajravelu, and M. M. Rashidi, "Forced convection heat transfer in a semi annulus under the influence of a variable magnetic field," *International journal of heat and mass transfer*, vol. 92, pp. 339–348, 2016.

[28] M. Sheikholeslami, R.-u. Haq, A. Shafee, and Z. Li, "Heat transfer behavior of nanoparticle enhanced PCM solidification through an enclosure with V shaped fins," *International Journal of Heat and Mass Transfer*, vol. 130, pp. 1322–1342, 2019.

[29] M. Sheikholeslami, "New computational approach for exergy and entropy analysis of nanofluid under the impact of Lorentz force through a porous medium," *Computer Methods in Applied Mechanics and Engineering*, vol. 344, pp. 319–333, 2019.

[30] M. Rashidi, M. Ali, N. Freidoonimehr, and F. Nazari, "Parametric analysis and optimization of entropy generation in unsteady MHD flow over a stretching rotating disk using artificial neural network and particle swarm optimization algorithm," *Energy*, vol. 55, pp. 497–510, 2013.

[31] M. Sheikholeslami, "Numerical approach for MHD Al_2O_3-water nanofluid transportation inside a permeable medium using innovative computer method," *Computer Methods in Applied Mechanics and Engineering*, vol. 344, pp. 306–318, 2019.

[32] M. Rashidi, N. Kavyani, and S. Abelman, "Investigation of entropy generation in MHD and slip flow over a rotating porous disk with variable properties," *International Journal of Heat and Mass Transfer*, vol. 70, pp. 892–917, 2014.

[33] M. Sheikholeslami, "Influence of magnetic field on Al_2O_3-H_2O nanofluid forced convection heat transfer in a porous lid driven cavity with hot sphere obstacle by means of LBM," *Journal of Molecular Liquids*, vol. 263, pp. 472–488, 2018.

[34] M. Sheikholeslami, S. Shehzad, Z. Li, and A. Shafee, "Numerical modeling for alumina nanofluid magnetohydrodynamic convective heat transfer in a permeable medium using Darcy law," *International Journal of Heat and Mass Transfer*, vol. 127, pp. 614–622, 2018.

[35] M. Sheikholeslami, "Application of Darcy law for nanofluid flow in a porous cavity under the impact of Lorentz forces," *Journal of Molecular Liquids*, vol. 266, pp. 495–503, 2018.

[36] A. M. Siddiqui, S. Irum, and A. R. Ansari, "Unsteady squeezing flow of a viscous MHD fluid between parallel plates, a solution using the Homotopy Perturbation Method," *Mathematical Modelling and Analysis*, vol. 13, no. 4, pp. 565–576, 2008.

[37] G. Domairry and A. Aziz, "Approximate analysis of MHD squeeze flow between two parallel disks with suction or injection by Homotopy Perturbation Method," *Mathematical Problems in Engineering*, vol. 2009, 2009.

[38] R. U. Haq, S. Nadeem, Z. Khan, and N. Noor, "MHD squeezed flow of water functionalized metallic nanoparticles over a sensor surface," *Physica E: Low-dimensional Systems and Nanostructures*, vol. 73, pp. 45–53, 2015.

[39] T. Hayat, R. Sajjad, A. Alsaedi, T. Muhammad, and R. Ellahi, "On squeezed flow of couple stress nanofluid between two parallel plates," *Results in physics*, vol. 7, pp. 553–561, 2017.

[40] B. Olajuwon, "Convection heat and mass transfer in a hydromagnetic flow of a second grade fluid in the presence of thermal radiation and thermal diffusion," *International Communications in Heat and Mass Transfer*, vol. 38, no. 3, pp. 377–382, 2011.

[41] S. Nadeem, R. U. Haq, N. S. Akbar, and Z. H. Khan, "MHD three-dimensional Casson fluid flow past a porous linearly stretching sheet," *Alexandria Engineering Journal*, vol. 52, no. 4, pp. 577–582, 2013.

[42] M. Hatami, D. Jing, D. Song, M. Sheikholeslami, and D. Ganji, "Heat transfer and flow analysis of nanofluid flow between parallel plates in presence of variable magnetic field using Homotopy Perturbation Method," *Journal of Magnetism and Magnetic Materials*, vol. 396, pp. 275–282, 2015.

[43] A. Rashad, M. Rashidi, G. Lorenzini, S. E. Ahmed, and A. M. Aly, "Magnetic field and internal heat generation effects on the free convection in a rectangular cavity filled with a porous medium saturated with Cu–water nanofluid," *International Journal of Heat and Mass Transfer*, vol. 104, pp. 878–889, 2017.

[44] C. Kirubhashankar and S. Ganesh, "Unsteady mhd flow of a casson fluid in a parallel plate channel with heat and mass transfer of chemical reaction," *Indian Journal of Research (3)*, pp. 101–105, 2014.

[45] C. Raju and N. Sandeep, "Heat and mass transfer in mhd non-newtonian bio-convection flow over a rotating cone/plate with cross diffusion," *Journal of molecular liquids*, vol. 215, pp. 115–126, 2016.

[46] X. Su and Y. Yin, "Effects of an inclined magnetic field on the unsteady squeezing flow between parallel plates with suction/injection," *Journal of Magnetism and Magnetic Materials*, vol. 484, pp. 266–271, 2019.

[47] J. H. Ferziger and M. Peric, *Computational Methods for Fluid Dynamics*. Springer Science & Business Media, 2012.

[48] Y. Cencel and J. Cimbala, *Fluid Mechanics, Fundamentals and Applications*. McGraw-Hill Internat. Ed., 2006.

[49] D. J. Tritton, *Physical Fluid Dynamics*. Springer Science & Business Media, 2012.

[50] F. M. White, *Fluid Mechanics*. McGraw-Hill, New York, 2003.

[51] R. Bansal, *A Textbook of Fluid Mechanics and Hydraulic Machines*. Laxmi Publications, 2004.

[52] G. G. T. Papanastasiou and A. N. Alexandrou, *Viscous Fluid Flow*. CRC press, 1999.

[53] F. M. White and I. Corfield, *Viscous Fluid Flow*, vol. 3. McGraw-Hill New York, 2006.

[54] J. Kunes, *Dimensionless Physical Quantities in Science and Engineering*. Elsevier, 2012.

[55] T. Y. Na, *Computational methods in engineering boundary value problems*. Academic Press, 1980.